US 20170187125A1

(19) **United States**

(12) **Patent Application Publication**

(10) **Pub. No.: US 2017/0187125 A1**

(43) **Pub. Date: Jun. 29, 2017**

ASHRAFI et al.

(54) **PATCH ANTENNA ARRAY FOR TRANSMISSION OF HERMITE-GAUSSIAN AND LAGUERRE GAUSSIAN BEAMS**

(71) Applicant: **NXGEN PARTNERS IP, LLC**, Dallas, TX (US)

(72) Inventors: **SOLYMAN ASHRAFI**, Plano, TX (US); **ROGER D. LINQUIST**, Dallas, TX (US)

(21) Appl. No.: **15/457,444**

(22) Filed: **Mar. 13, 2017**

Related U.S. Application Data

(63) Continuation of application No. 15/187,315, filed on Jun. 20, 2016, now Pat. No. 9,595,766.

(60) Provisional application No. 62/182,227, filed on Jun. 19, 2015, provisional application No. 62/233,838, filed on Sep. 28, 2015, provisional application No. 62/242,056, filed on Oct. 15, 2015, provisional application No. 62/311,633, filed on Mar. 22, 2016.

Publication Classification

(51) **Int. Cl.**

H01Q 21/06	(2006.01)
H01Q 3/26	(2006.01)
H01Q 15/16	(2006.01)

(52) **U.S. Cl.**

CPC ***H01Q 21/065*** (2013.01); ***H01Q 15/16*** (2013.01); ***H01Q 3/26*** (2013.01)

(57) **ABSTRACT**

An antenna array includes a plurality of patch antennas including a plurality of layers. Each of the plurality of layers are separated by a distance and each support a portion of the plurality of patch antennas. A plurality of connectors are each associated with one of the plurality of layers and supply a signal for transmission by the associated layer. A feed network on each of the plurality of layers provides a connection between a connector associated with the layer and the portion of the patch antennas located on the layer. Each layer transmits a signal having a different orthogonal function applied thereto that multiplexes each of the signals having a different orthogonal function applied thereto onto a single transmission beam. A parabolic reflector reflects the single transmission beam from the plurality of layers of the antenna array.

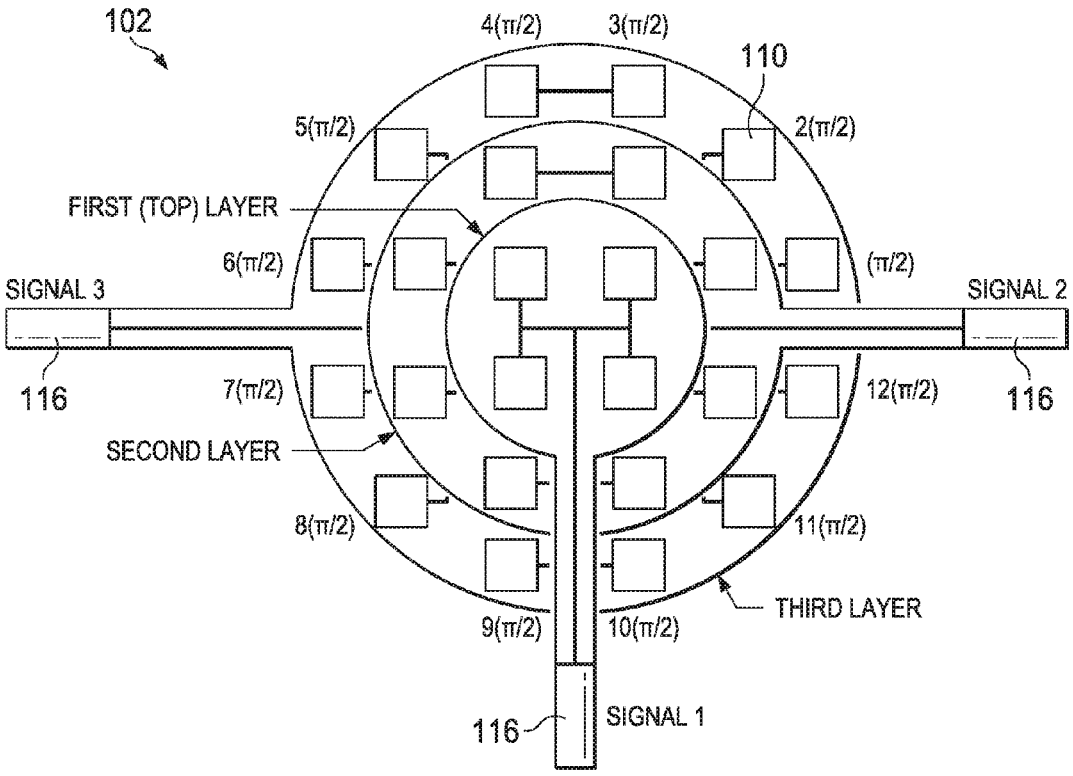

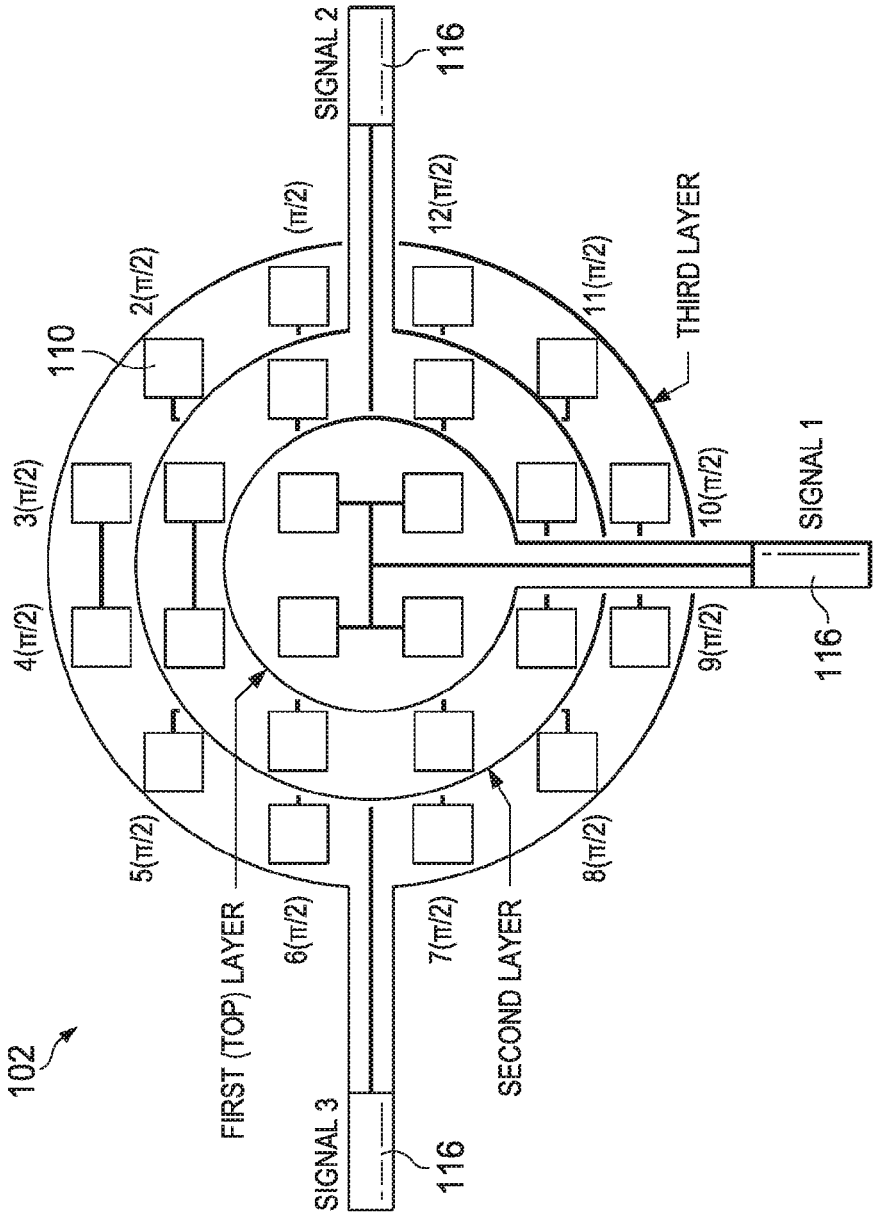
102
110
SIGNAL 2
116
SIGNAL 1
116
SIGNAL 3
116
FIRST (TOP) LAYER
SECOND LAYER
THIRD LAYER
(π/2)
2(π/2)
3(π/2)
4(π/2)
5(π/2)
6(π/2)
7(π/2)
8(π/2)
9(π/2)
10(π/2)
11(π/2)
12(π/2)

FIG. 1

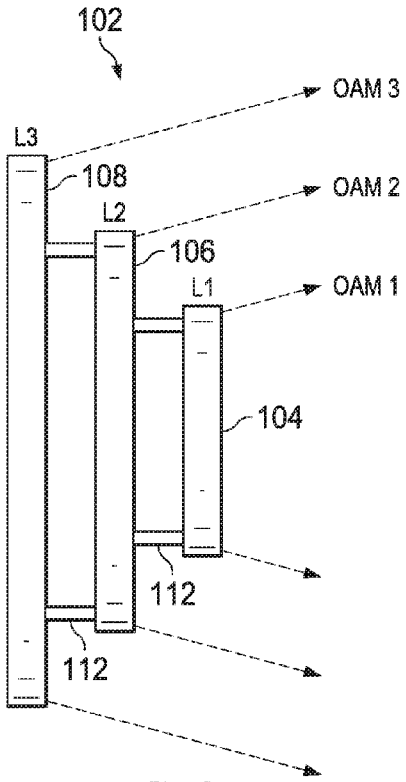

FIG. 2

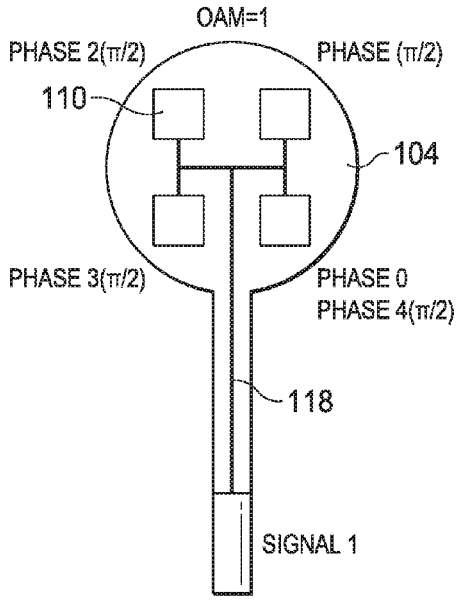

FIG. 3

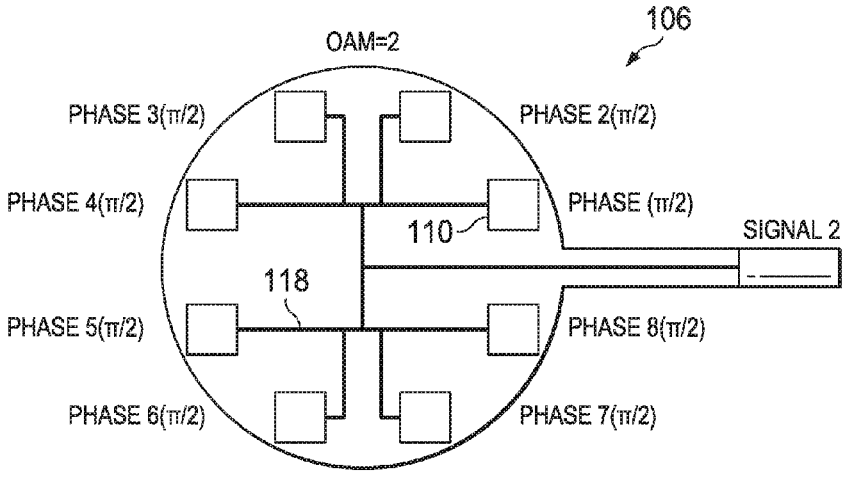

FIG. 4

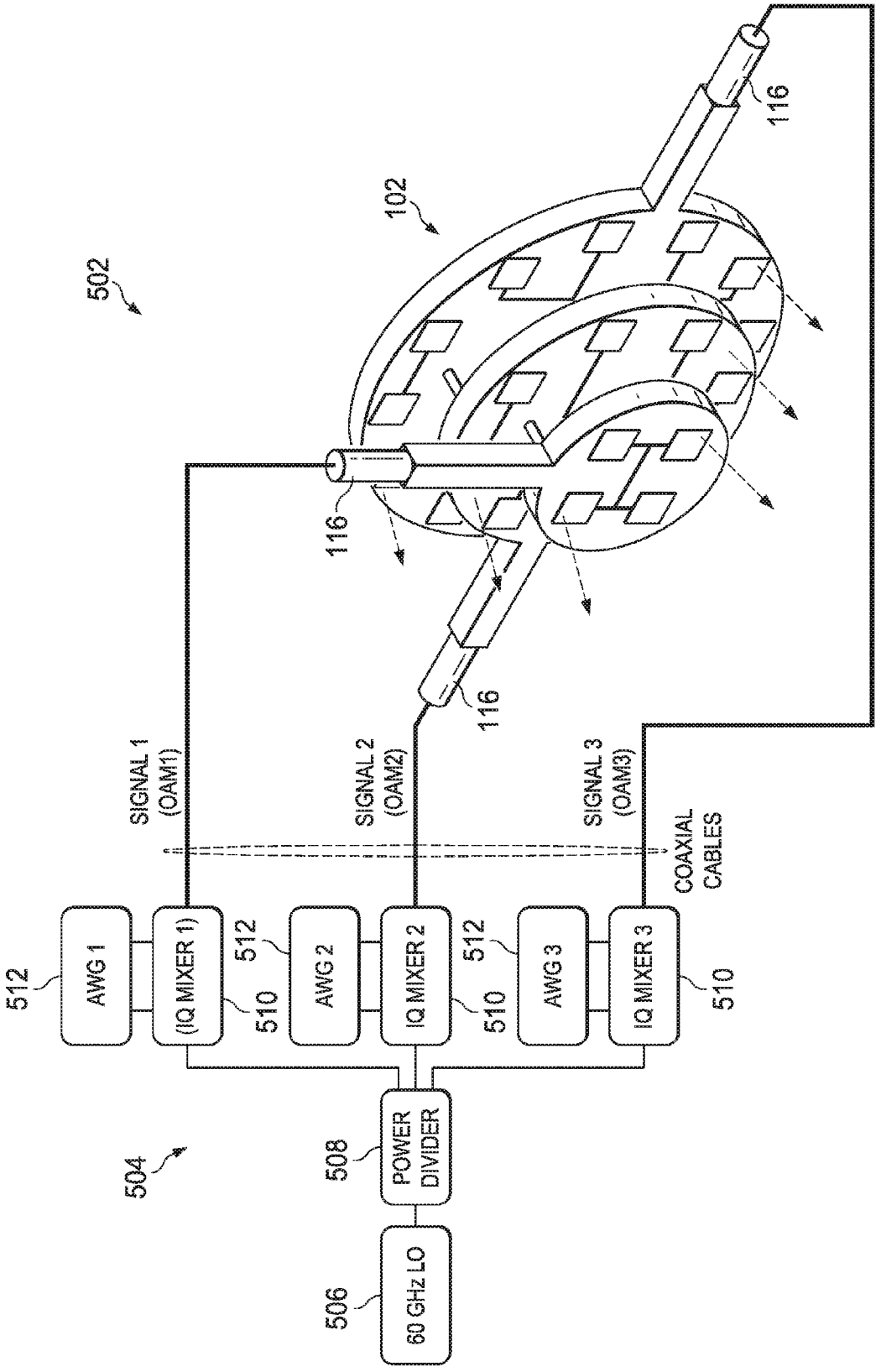
502
102
116
116
116
SIGNAL 1 (OAM1)
SIGNAL 2 (OAM2)
SIGNAL 3 (OAM3)
COAXIAL CABLES
512
AWG 1
(IQ MIXER 1)
510
512
AWG 2
IQ MIXER 2
510
512
AWG 3
IQ MIXER 3
510
504
508
POWER DIVIDER
506
60 GHz LO

FIG. 5

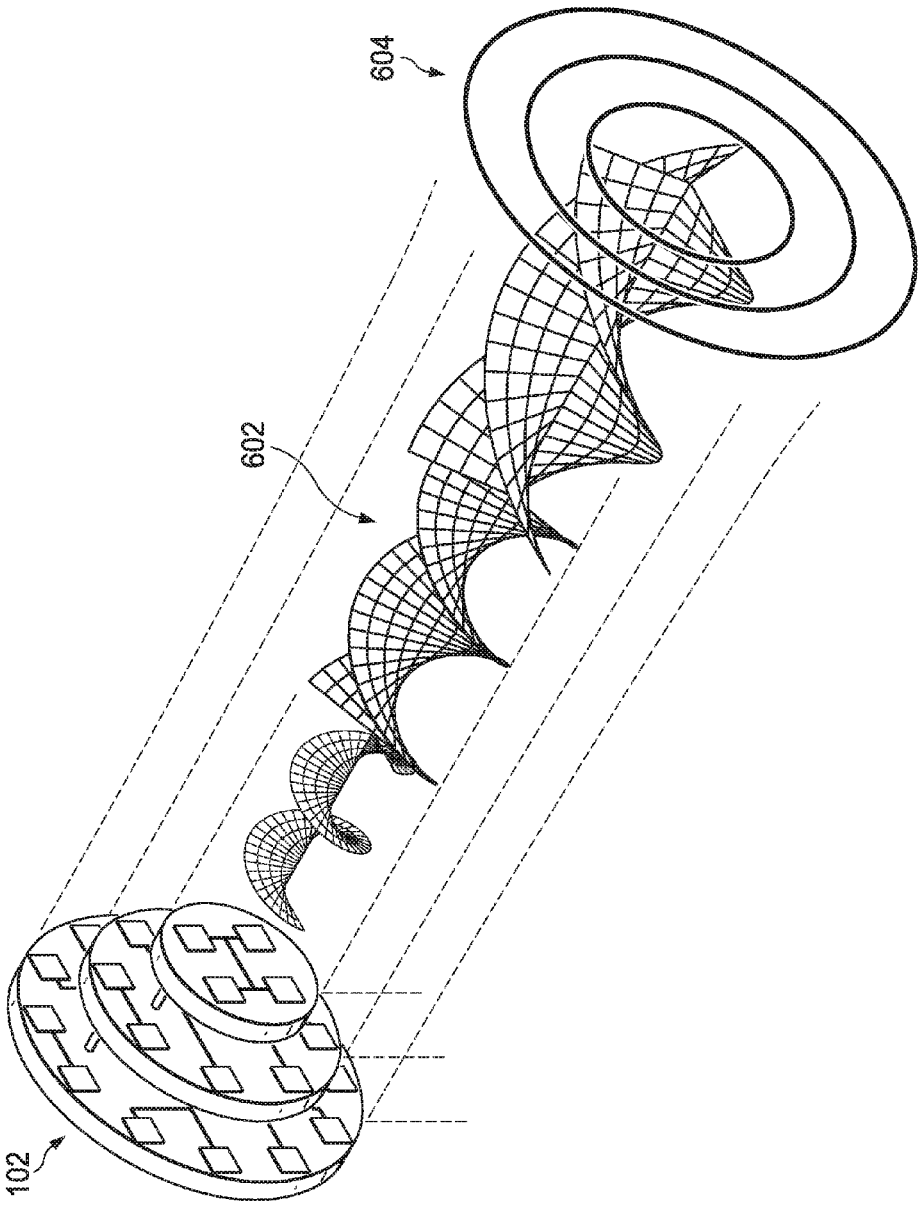

FIG. 6

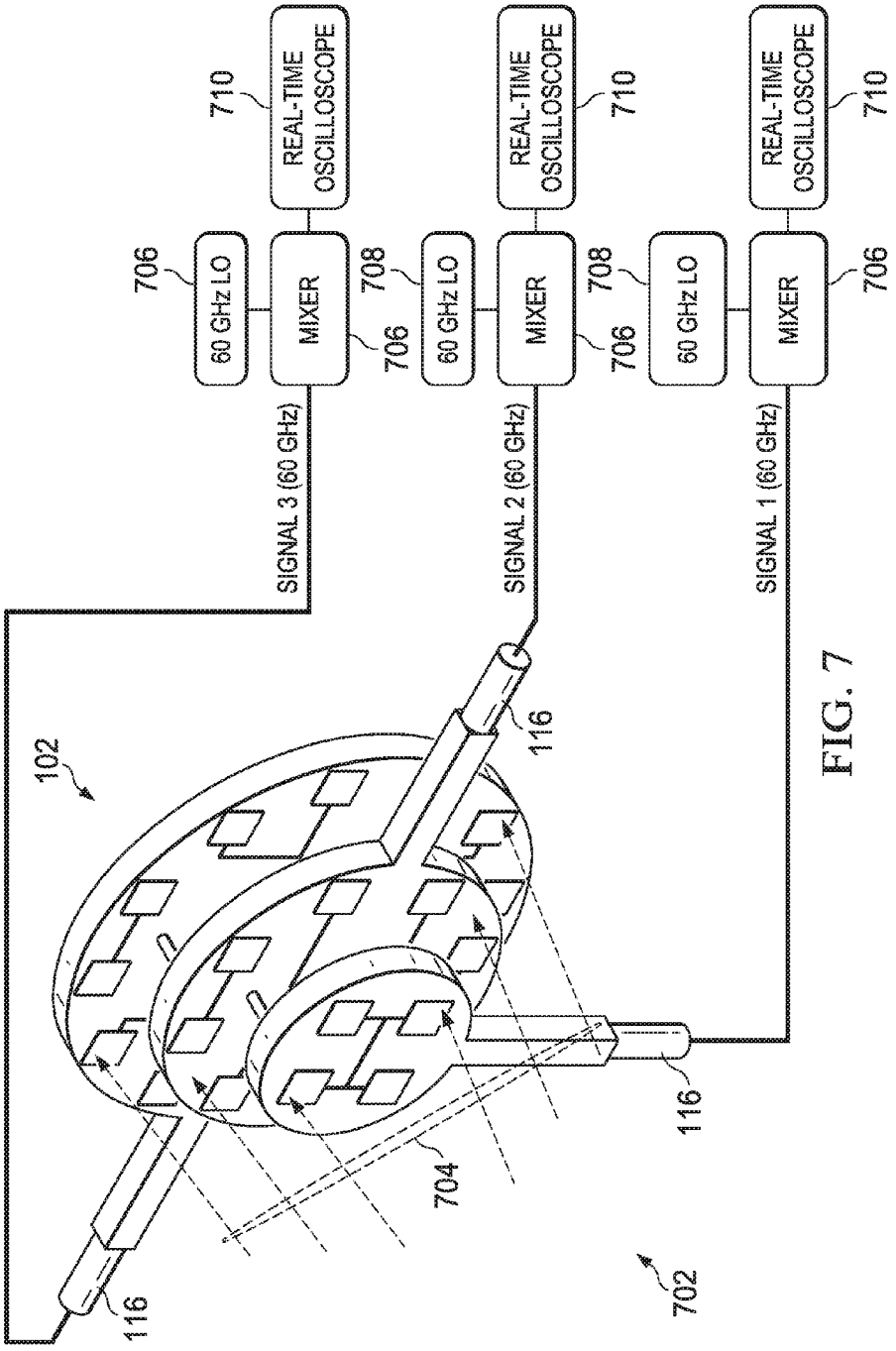
710
REAL-TIME OSCILLOSCOPE
706
60 GHz LO
MIXER
708
706
SIGNAL 3 (60 GHz)
SIGNAL 2 (60 GHz)
SIGNAL 1 (60 GHz)
102
116
704
702

FIG. 7

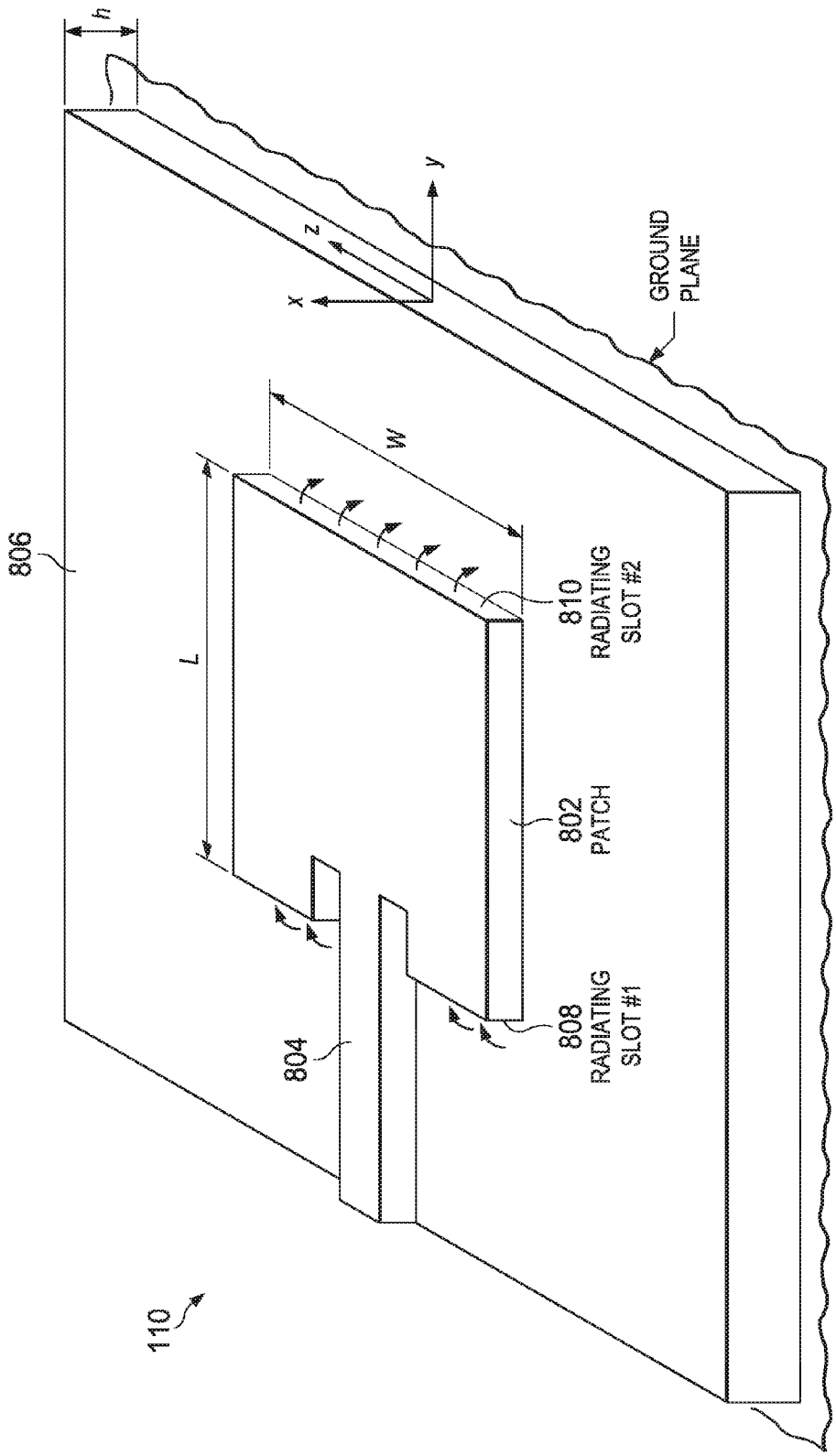
h
y
z
x
GROUND PLANE
W
L
806
810
RADIATING SLOT #2
802
PATCH
808
RADIATING SLOT #1
804
110

FIG. 8

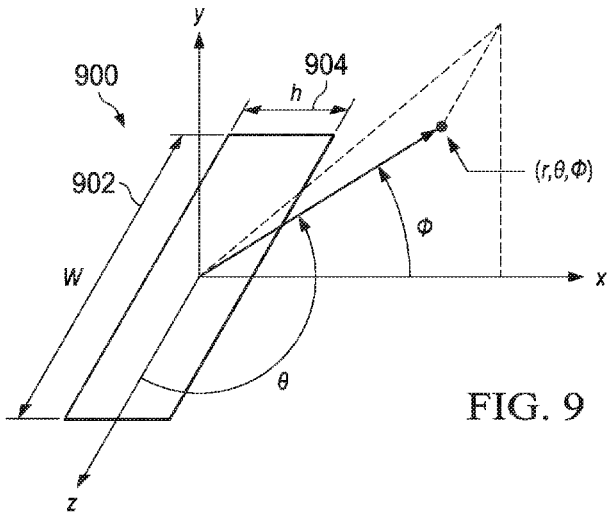

FIG. 9

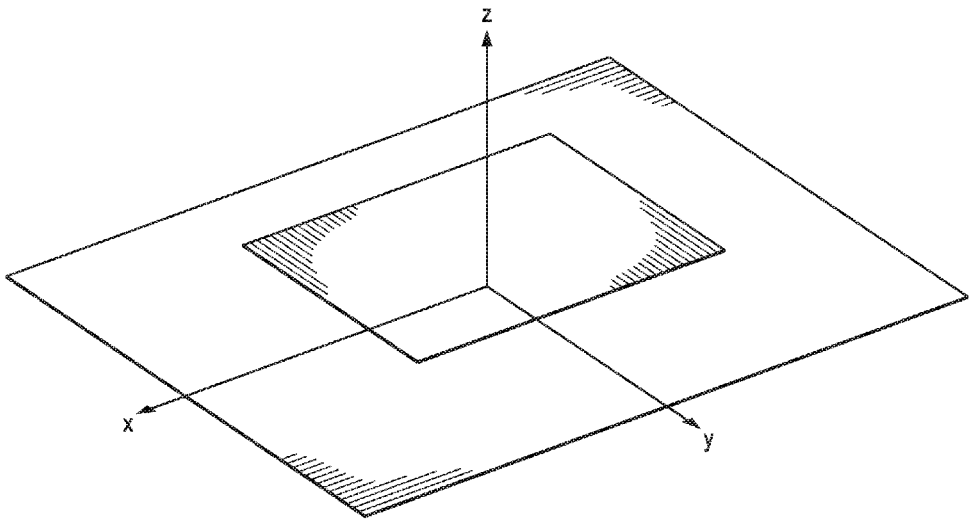

FIG. 10

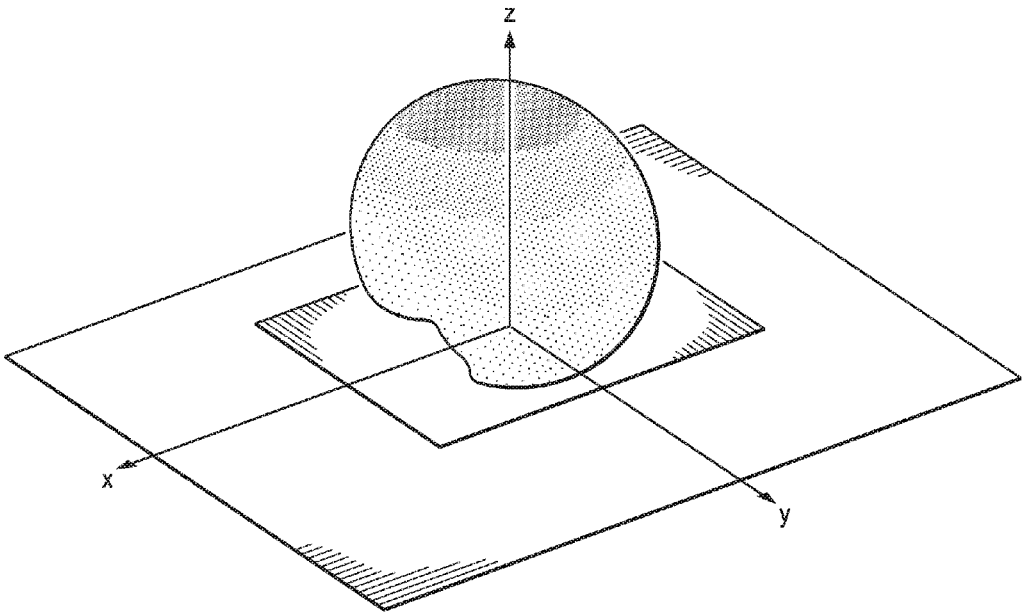

FIG. 11

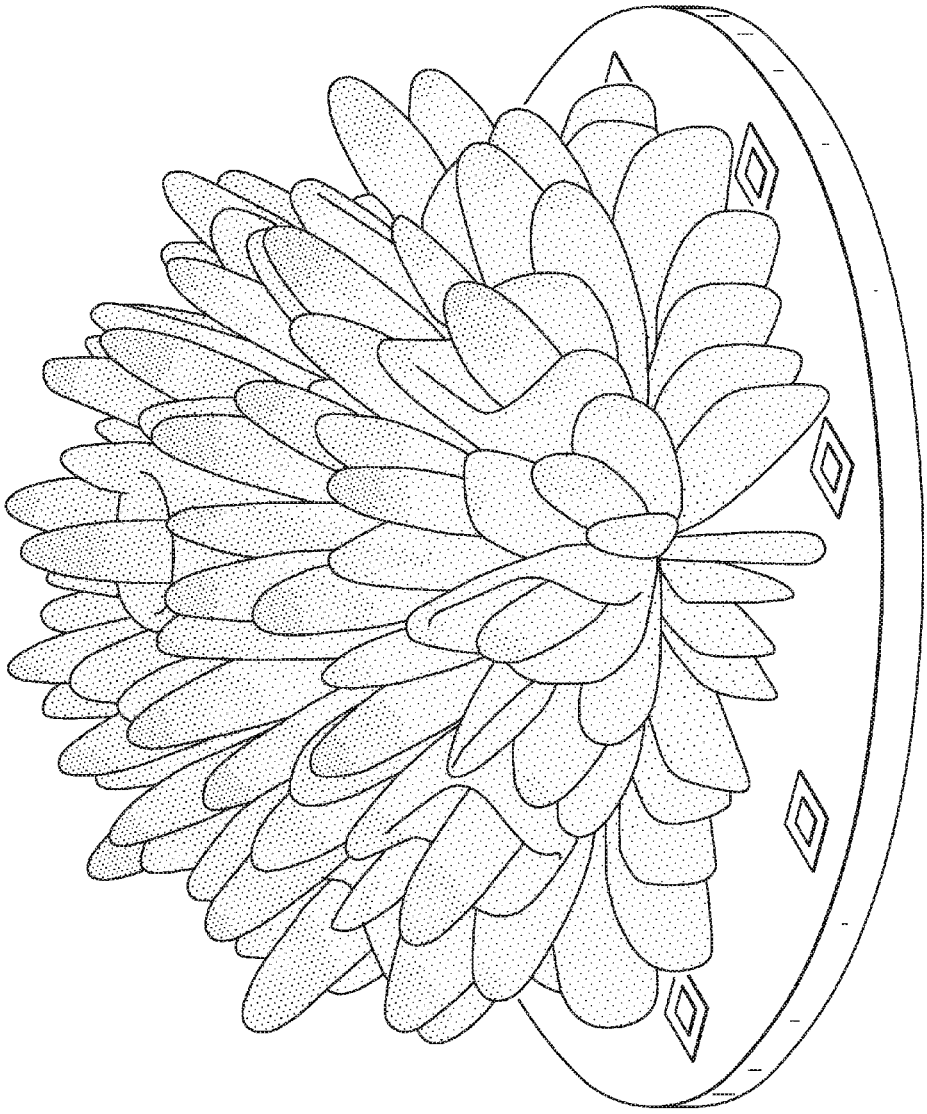

FIG. 12a

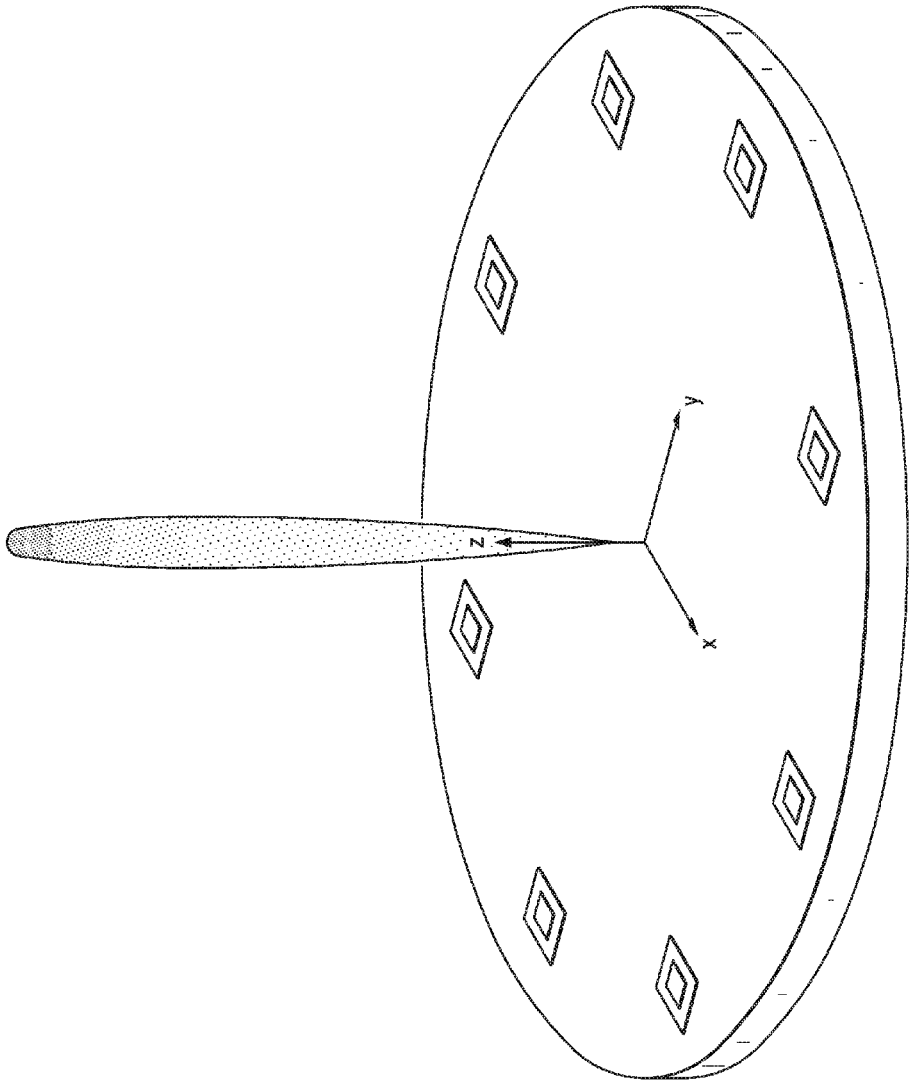

FIG. 12b

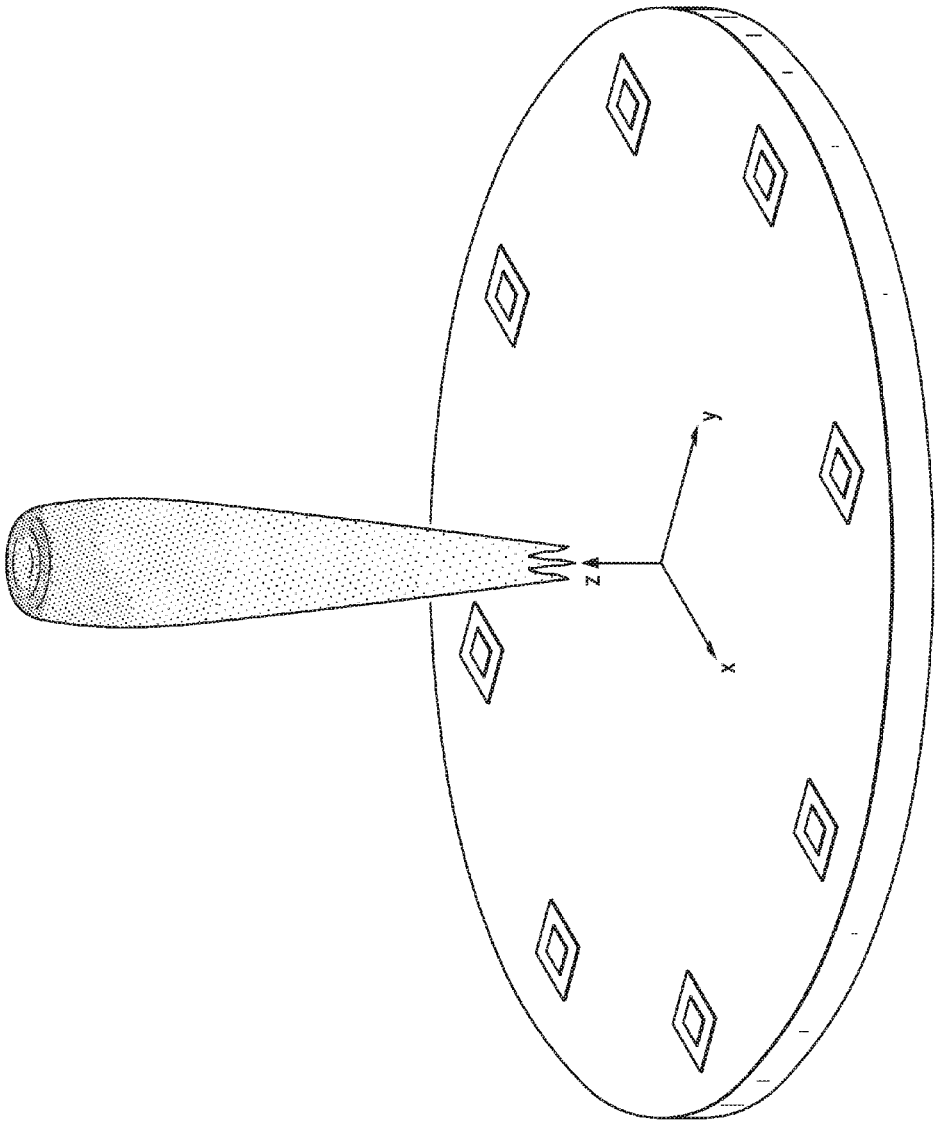

FIG. 12c

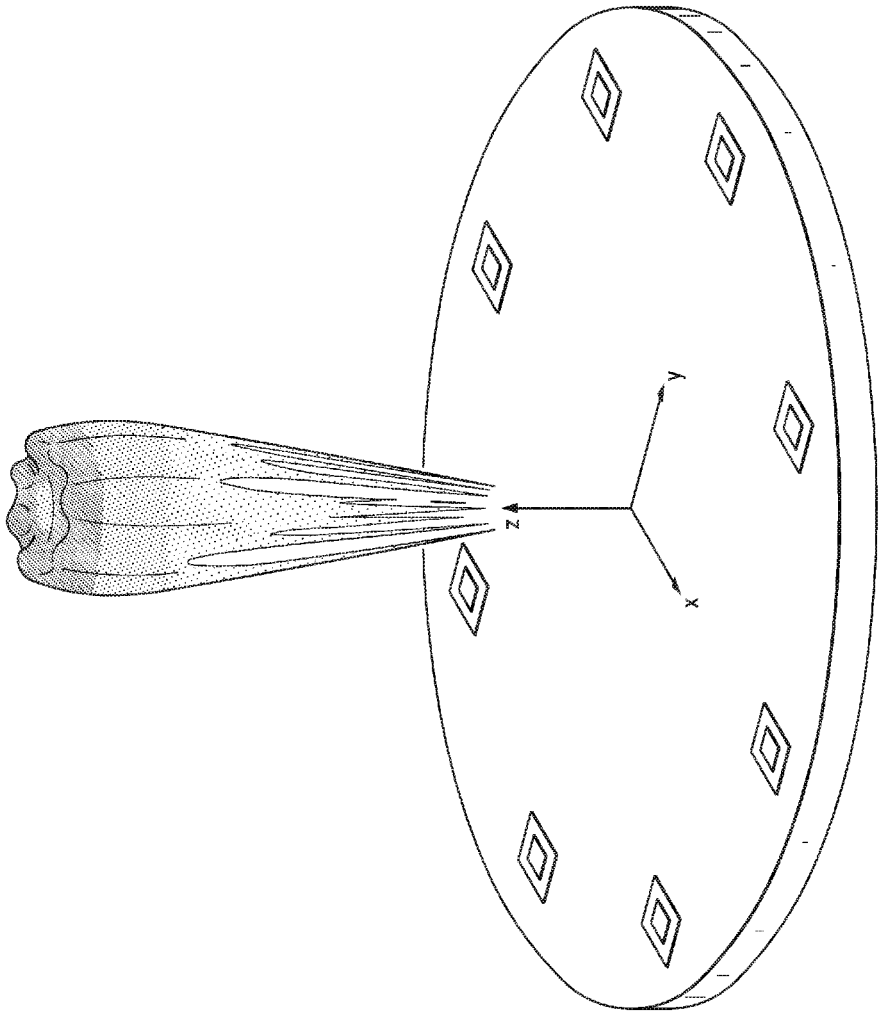

FIG. 12d

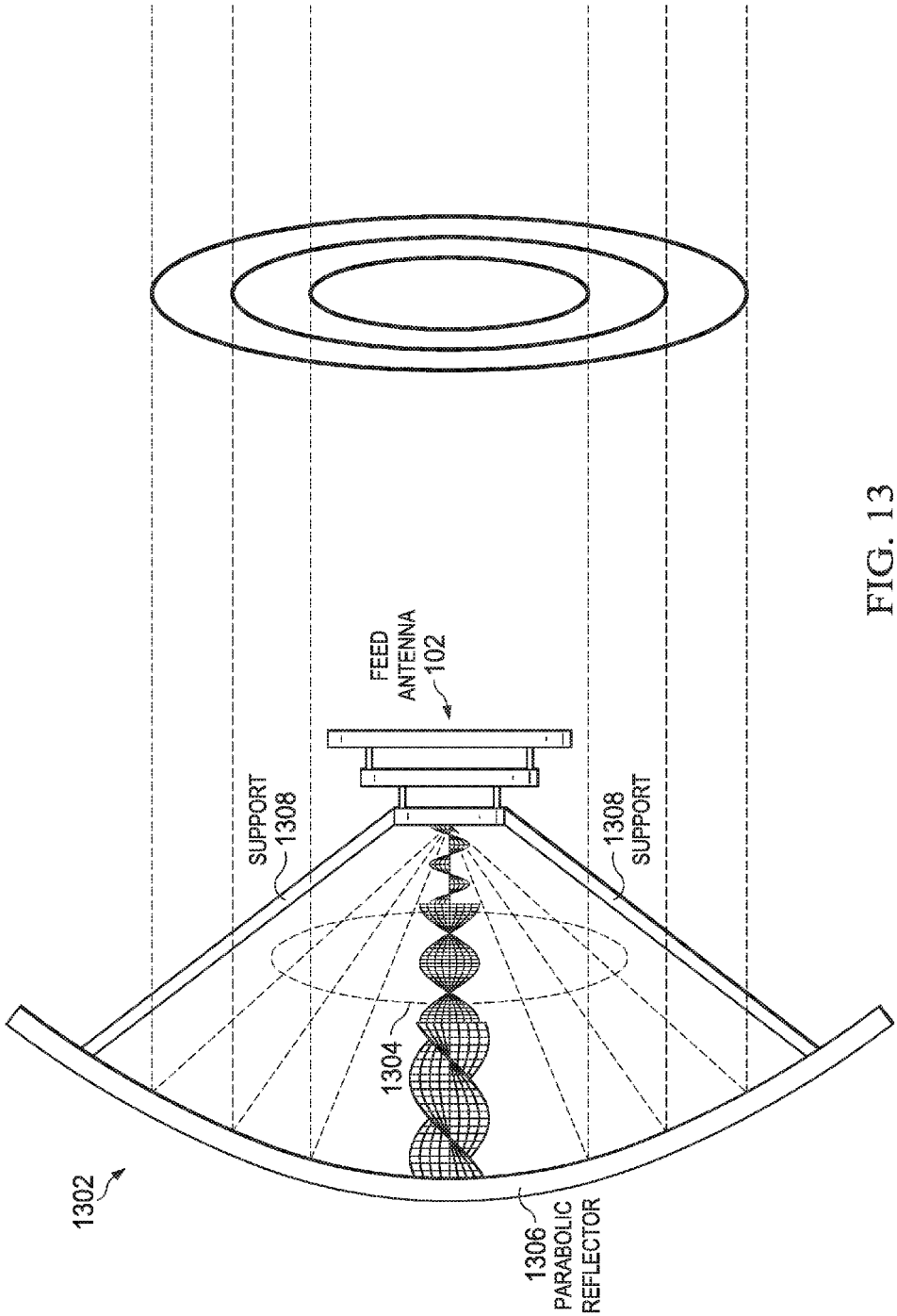
1302
1306
PARABOLIC
REFLECTOR
1304
SUPPORT
1308
SUPPORT
1308
FEED
ANTENNA
102

FIG. 13

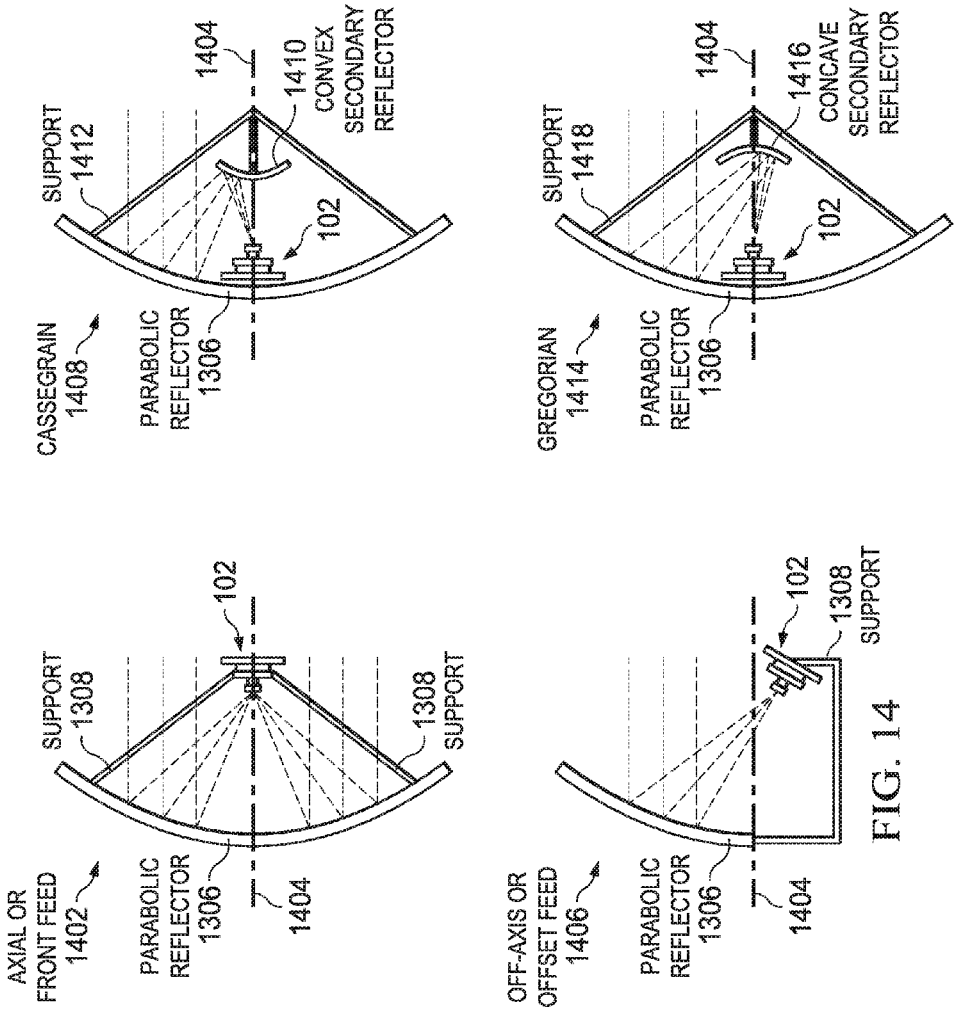
CASSEGRAIN
1408
PARABOLIC
REFLECTOR
1306
SUPPORT
1412
1404
1410
CONVEX
SECONDARY
REFLECTOR
102
GREGORIAN
1414
PARABOLIC
REFLECTOR
1306
SUPPORT
1418
1404
1416
CONCAVE
SECONDARY
REFLECTOR
102
AXIAL OR
FRONT FEED
1402
PARABOLIC
REFLECTOR
1306
SUPPORT
1308
102
1404
1308
SUPPORT
OFF-AXIS OR
OFFSET FEED
1406
PARABOLIC
REFLECTOR
1306
102
1308
SUPPORT
1404

FIG. 14

FIG. 15

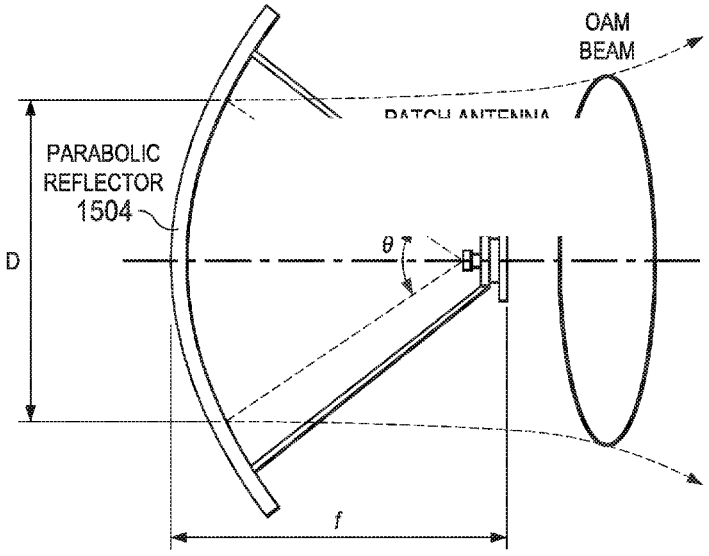
OAM
BEAM
PARABOLIC
REFLECTOR
1504
D
θ
f

FIG. 16

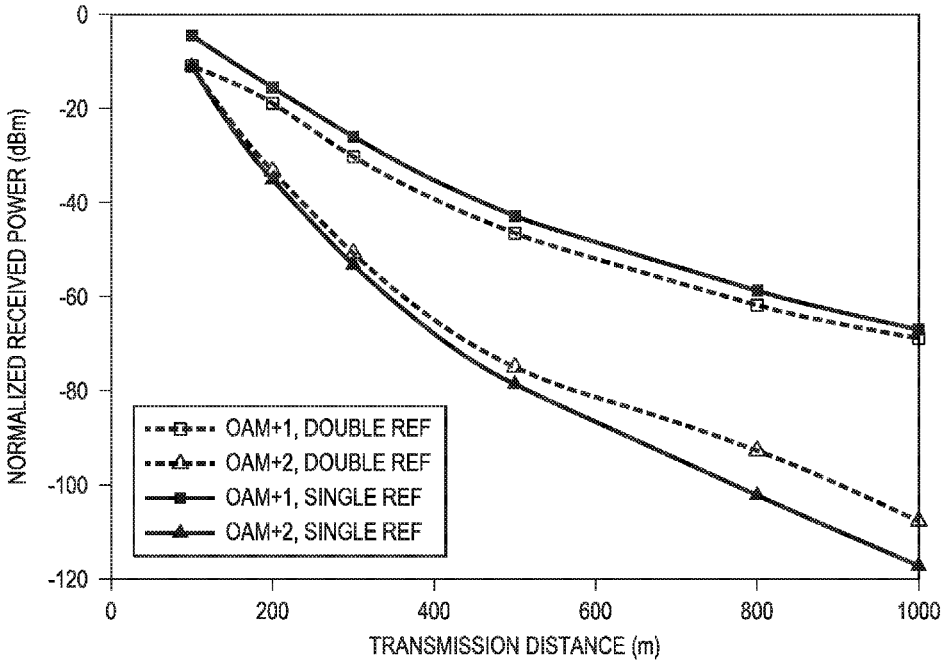
NORMALIZED RECEIVED POWER (dBm)
0
-20
-40
-60
-80
-100
-120
0
200
400
600
800
1000
TRANSMISSION DISTANCE (m)
OAM+1, DOUBLE REF
OAM+2, DOUBLE REF
OAM+1, SINGLE REF
OAM+2, SINGLE REF

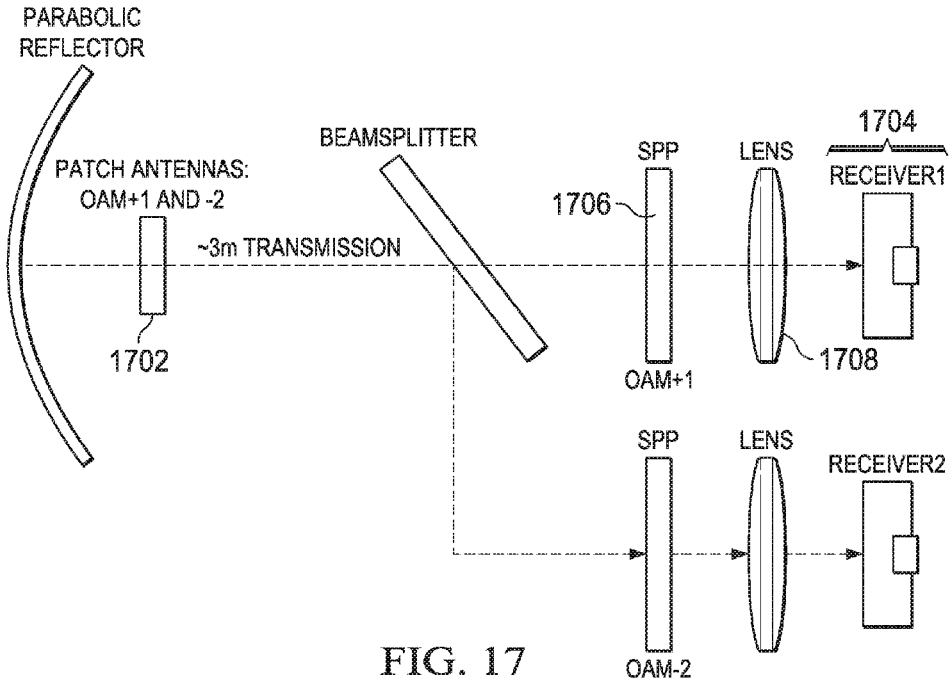
PARABOLIC REFLECTOR
PATCH ANTENNAS: OAM+1 AND -2
~3m TRANSMISSION
1702
BEAMSPLITTER
SPP
1706
OAM+1
LENS
1704
RECEIVER1
1708
SPP
OAM-2
LENS
RECEIVER2

FIG. 17

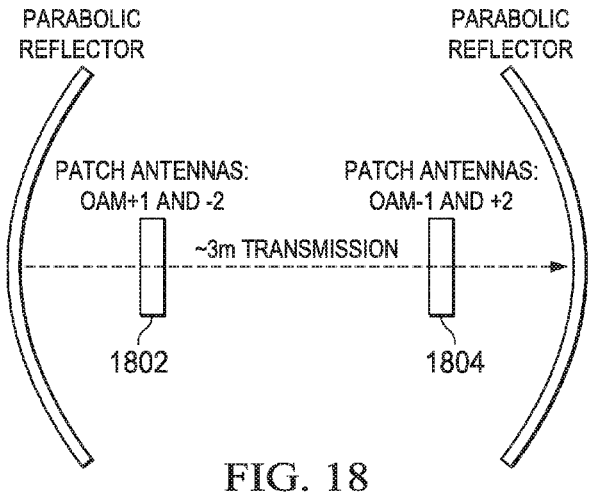
PARABOLIC REFLECTOR
PARABOLIC REFLECTOR
PATCH ANTENNAS: OAM+1 AND -2
PATCH ANTENNAS: OAM-1 AND +2
~3m TRANSMISSION
1802
1804

FIG. 18

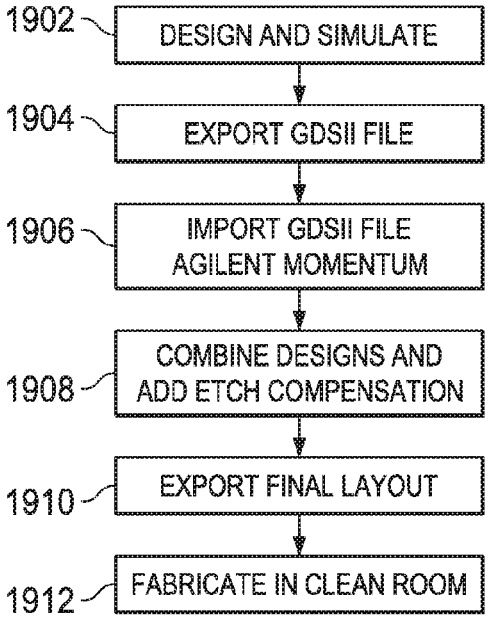
1902
DESIGN AND SIMULATE
1904
EXPORT GDSII FILE
1906
IMPORT GDSII FILE
AGILENT MOMENTUM
1908
COMBINE DESIGNS AND
ADD ETCH COMPENSATION
1910
EXPORT FINAL LAYOUT
1912
FABRICATE IN CLEAN ROOM

FIG. 19

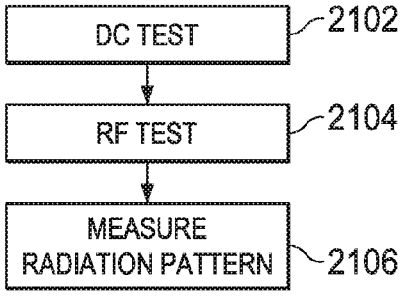
DC TEST
2102
RF TEST
2104
MEASURE
RADIATION PATTERN
2106

FIG. 21

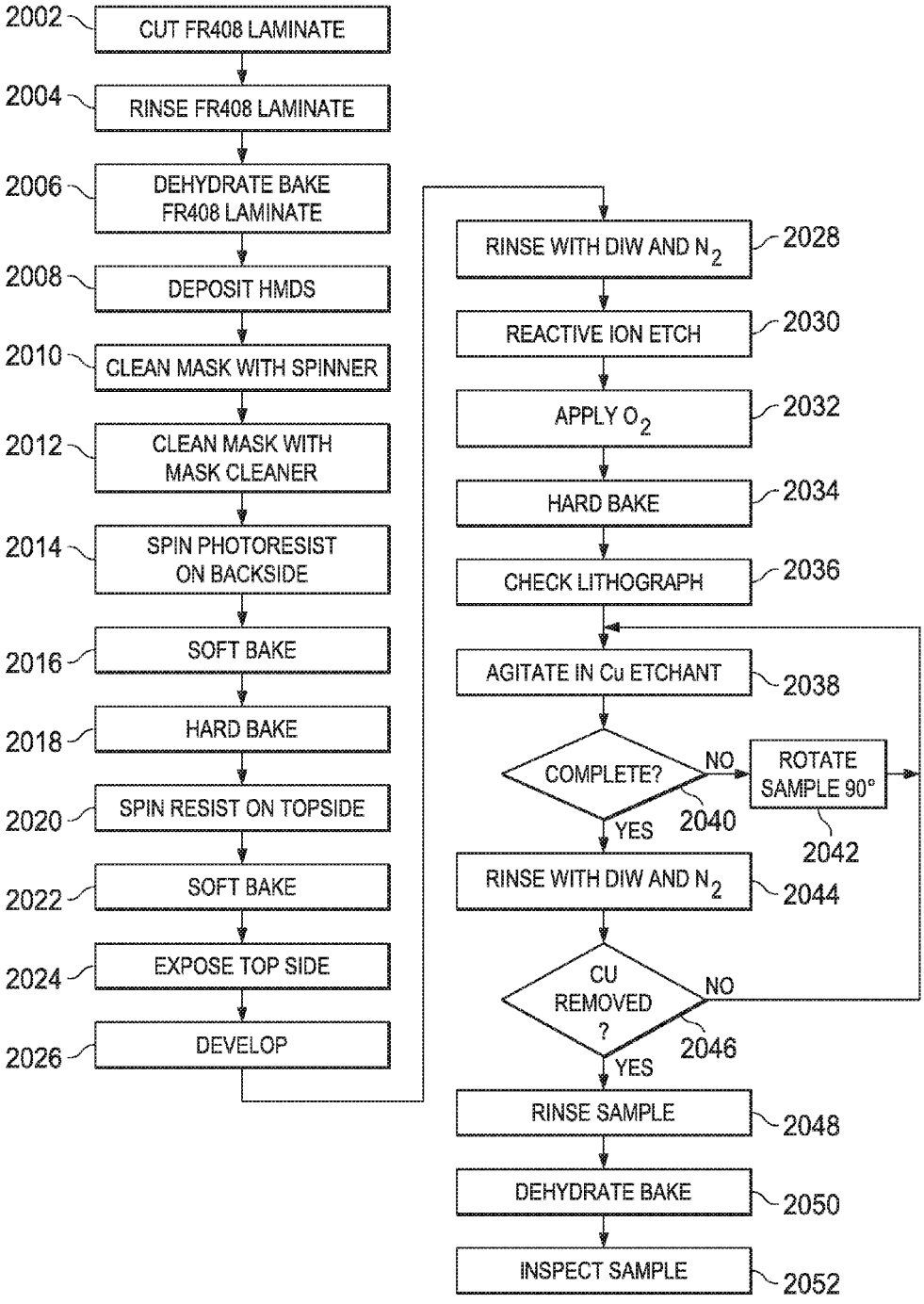
2002
CUT FR408 LAMINATE
2004
RINSE FR408 LAMINATE
2006
DEHYDRATE BAKE FR408 LAMINATE
2008
DEPOSIT HMDS
2010
CLEAN MASK WITH SPINNER
2012
CLEAN MASK WITH MASK CLEANER
2014
SPIN PHOTORESIST ON BACKSIDE
2016
SOFT BAKE
2018
HARD BAKE
2020
SPIN RESIST ON TOPSIDE
2022
SOFT BAKE
2024
EXPOSE TOP SIDE
2026
DEVELOP
RINSE WITH DIW AND N_2
2028
REACTIVE ION ETCH
2030
APPLY O_2
2032
HARD BAKE
2034
CHECK LITHOGRAPH
2036
AGITATE IN Cu ETCHANT
2038
COMPLETE?
NO
ROTATE SAMPLE 90°
2042
YES
2040
RINSE WITH DIW AND N_2
2044
CU REMOVED ?
NO
YES
2046
RINSE SAMPLE
2048
DEHYDRATE BAKE
2050
INSPECT SAMPLE
2052

FIG. 20

PATCH ANTENNA ARRAY FOR TRANSMISSION OF HERMITE-GAUSSIAN AND LAGUERRE GAUSSIAN BEAMS

CROSS-REFERENCE TO RELATED APPLICATIONS

[0001] This application is a continuation application of U.S. patent application Ser. No. 15/187,315, filed Jun. 20, 2016, entitled PATCH ANTENNA ARRAY FOR TRANSMISSION OF HERMITE-GAUSSIAN AND LAGUERRE GAUSSIAN BEAMS (Atty. Dkt. No. NXGN-33142), which claims priority to U.S. Provisional Application No. 62/182,227, entitled PATCH ANTENNAS FOR TRANSMISSION OF HERMITE-GAUSSIAN AND LAGUERRE-GAUSSIAN BEAMS, filed on Jun. 19, 2015 (Atty. Docket No. NXGN-32702); U.S. Provisional No. 62/233,838, entitled PATCH ANTENNAS FOR TRANSMISSION OF HERMITE-GAUSSIAN AND LAGUERRE-GAUSSIAN BEAMS, filed on Sep. 28, 2015 (Atty. Docket No. NXGN-32812); U.S. Provisional Application No. 62/242,056, entitled METHOD FOR MANUFACTURING A PATCH ANTENNA, filed on Oct. 15, 2015 (Atty. Docket No. NXGN-32844); and U.S. Provisional Application No. 62/311,633, entitled HYBRID PATCH ANTENNA WITH PARABOLIC REFLECTOR, filed on Mar. 22, 2016 (Atty. Docket No. NXGN-33052), each of which is incorporated herein by reference in their entirety.

TECHNICAL FIELD

[0002] The present application relates to patch antennas, and more particularly to patch antennas for the transmission of Hermite-Gaussian and Laguerre-Gaussian Beams.

BACKGROUND

[0003] When transmitting Hermite-Gaussian and Laguerre-Gaussian beams, the ability to multiplex multiple modes of these type of beams together into a single signal is needed to provide increased bandwidth. By increasing the number of Hermite-Gaussian and Laguerre-Gaussian beams that can be multiplexed together, an increased data throughput can be achieved. Thus, there is a need for antenna and transmission structures that provide for multiplexing of Hermite-Gaussian and Laguerre-Gaussian beams.

SUMMARY

[0004] The present invention, as disclosed and described herein, in one aspect thereof comprises a multi-level antenna array including a plurality of patch antennas. The antenna further includes a plurality of layers. Each of the plurality of layers are separated from each other by a distance and each of the plurality of layers further support a portion of the plurality of patch antennas. A plurality of connectors are each associated with one of the plurality of layers and supply a signal for transmission by the associated layer. A feed network on each of the plurality of layers provides a connection between a connector of the plurality of connectors associated with the layer and the portion of the plurality of patch antennas located on the layer. Each layer of the plurality of layers transmits the signal having a different orthogonal function applied thereto that multiplexes each of the signals having a different orthogonal function applied thereto onto a single transmission beam. A parabolic reflector reflects the single transmission beam from the plurality of layers of the multi-level antenna array.

BRIEF DESCRIPTION OF THE DRAWINGS

[0005] For a more complete understanding, reference is now made to the following description taken in conjunction with the accompanying Drawings in which:

[0006] FIG. **1** illustrates a top view of a multilayer patch antenna array;

[0007] FIG. **2** illustrates a side view of a multilayer patch antenna array;

[0008] FIG. **3** illustrates a first layer of a multilayer patch antenna array;

[0009] FIG. **4** illustrates a second layer of a multilayer patch antenna array;

[0010] FIG. **5** illustrates a transmitter for use with a multilayer patch antenna array;

[0011] FIG. **6** illustrates a multiplexed OAM signal transmitted from a multilayer patch antenna array;

[0012] FIG. **7** illustrates a receiver for use with a multilayer patch antenna array;

[0013] FIG. **8** illustrates a microstrip patch antenna;

[0014] FIG. **9** illustrates a coordinate system for an aperture of a microstrip patch antenna;

[0015] FIG. **10** illustrates a 3-D model of a single rectangular patch antenna;

[0016] FIG. **11** illustrates the radiation pattern of the patch antenna of FIG. **10**;

[0017] FIG. **12***a* illustrates the radiation pattern of a circular array for an OAM mode order 1=0;

[0018] FIG. **12***b* illustrates the radiation pattern for an OAM mode order 1=0 in the vicinity of the array axis;

[0019] FIG. **12***c* illustrates the radiation pattern for an OAM mode order 1=1 in the vicinity of the array axis;

[0020] FIG. **12***d* illustrates the radiation pattern for an OAM mode order 1=2 in the vicinity of the array axis;

[0021] FIG. **13** illustrates a multilayer patch antenna array with a parabolic reflector;

[0022] FIG. **14** illustrates various configurations of the patch antenna and parabolic reflector;

[0023] FIG. **15** illustrates a hybrid patch and parabolic antenna using a single reflector;

[0024] FIG. **16** illustrates the simulated results of received power as a function of transmission distance with a single reflection and double reflection hybrid patch and parabolic antenna;

[0025] FIG. **17** illustrates an OAM multiplexed link using hybrid patch and parabolic antenna with spiral phase plate at a receiver;

[0026] FIG. **18** illustrates an OAM multiplexed link using hybrid patch and parabolic antenna for the transmitter and the receiver;

[0027] FIG. **19** is a flow diagram illustrating the design and layout process of a patch antenna;

[0028] FIG. **20** is a flow diagram illustrating the process for patterning a copper layer on a laminate for a patch antenna; and

[0029] FIG. **21** is a flow diagram illustrating a testing process for a manufactured patch antenna.

DETAILED DESCRIPTION

[0030] Referring now to the drawings, wherein like reference numbers are used herein to designate like elements

throughout, the various views and embodiments of a patch antenna array for transmission of Hermite-Gaussian and Laguerre-Gaussian beams are illustrated and described, and other possible embodiments are described. The figures are not necessarily drawn to scale, and in some instances the drawings have been exaggerated and/or simplified in places for illustrative purposes only. One of ordinary skill in the art will appreciate the many possible applications and variations based on the following examples of possible embodiments.

[0031] FIG. **1** illustrates a multilayer patch antenna array **102**. The multilayer patch antenna array **102** includes a first antenna layer **104** for transmitting a first ordered beam, a second antenna layer **106** for transmitting a second ordered beam and a third layer **108** for transmitting a third ordered beam. Each of the layers **104**, **106** and **108** are stacked on a same center. While the present embodiment is illustrated with respect to a multilayer patch antenna array **102** including only three layers, it should be realized that either more or less layers may be implemented in a similar fashion as described herein. On the surface of each of the layers **104**, **106** and **108** are placed patch antennas **110**. Each of the patch antennas are placed such that they are not obscured by the above layer. The layers **104**, **106** and **108** are separated from each other by layer separator members **112** that provide spacing between each of the layers **104**, **106** and **108**. The configuration of the layers of the patch antenna may be in rectangular, circular or elliptical configurations to generate Hermite-Gaussian, Laguerre-Gaussian or Ince-Gaussian beams.

[0032] The patch antennas **110** used within the multilayer patch antenna array **102** are made from FR408 (flame retardant 408) laminate that is manufactured by Isola Global, of Chandler Ariz. and has a relative permittivity of approximately 3.75. The antenna has an overall height of 125 μm. The metal of the antenna is copper having a thickness of approximately 12 μm. The patch antenna is designed to have an operating frequency of 73 GHz and a free space wavelength of 4.1 mm. The dimensions of the input 50 Ohm line of the antenna is 280 μm while the input dimensions of the 100 Ohm line are 66 μm.

[0033] Each of the patch antennas **110** are configured to transmit signals at a predetermined phase that is different from the phase of each of the other patch antenna **110** on a same layer. Thus, as further illustrated in FIG. **3**, there are four patch antenna elements **110** included on a layer **104**. Each of the antenna elements **104** have a separate phase associated there with as indicated in FIG. **3**. These phases include $\pi/2$, $2(\pi/2)$, $3(\pi/2)$ and $4(\pi/2)$. Similarly, as illustrated in FIG. **4** layer **106** includes eight different patch antenna elements **110** including the phases $\pi/2$, $2(\pi/2)$, $3(\pi/2)$, $4(\pi/2)$, $5(\pi/2)$, $6(\pi/2)$, $7(\pi/2)$ and $8(\pi/2)$ as indicated. Finally, referring back to FIG. **1**, there are included 12 patch antenna elements **110** on layer **108**. Each of these patch antenna elements **110** have a phase assigned thereto in the manner indicated in FIG. **1**. These phases include $\pi/2$, $2(\pi/2)$, $3(\pi/2)$, $4(\pi/2)$, $5(\pi/2)$, $6(\pi/2)$, $7(\pi/2)$, $8(\pi/2)$, $9(\pi/2)$, $10(\pi/2)$, $11(\pi/2)$ and $12(\pi/2)$.

[0034] Each of the antenna layers **104**, **106** and **108** are connected to a coaxial end-launch connector **116** to feed each layer of the multilayer patch antenna array **102**. Each of the connectors **116** are connected to receive a separate signal that allows the transmission of a separate ordered antenna beam in a manner similar to that illustrated in FIG. **2**. The emitted beams are multiplexed together by the multilayered patch antenna array **102**. The orthogonal wavefronts transmitted from each layer of the multilayered patch antenna array **102** in a spatial manner to increase capacity as each wavefront will act as an independent Eigen channel. The signals are multiplexed onto a single frequency and propagate without interference or crosstalk between the multiplexed signals. While the illustration with respect to FIG. **2** illustrates the transmission of OAM beams at OAM 1, OAM 2 and OAM 3 ordered levels.

[0035] It should be understood that other types of Hermite Gaussian and Laguerre Gaussian beams can be transmitted using the multilayer patch antenna array **102** illustrated. Hermite-Gaussian polynomials and Laguerre-Gaussian polynomials are examples of classical orthogonal polynomial sequences, which are the Eigenstates of a quantum harmonic oscillator. However, it should be understood that other signals may also be used, for example orthogonal polynomials or functions such as Jacobi polynomials, Gegenbauer polynomials, Legendre polynomials and Chebyshev polynomials. Legendre functions, Bessel functions, prolate spheroidal functions and Ince-Gaussian functions may also be used. Q-functions are another class of functions that can be employed as a basis for orthogonal functions.

[0036] The feeding network **118** illustrated on each of the layers **104**, **106**, **108** uses delay lines of differing lengths in order to establish the phase of each patch antenna element **110**. By configuring the phases as illustrated in FIGS. **1-3** the OAM beams of different orders are generated and multiplexed together.

[0037] Referring now to FIG. **5**, there is illustrated a transmitter **502** for generating a multiplexed beam for transmission. As discussed previously, the multilayered patch antenna array **102** includes a connector **116** associated with each layer **104**, **106**, **108** of the multilayer patch antenna array **102**. Each of these connectors **116** are connected with signal generation circuitry **504**. The signal generation circuitry **504** includes, in one embodiment, a 60 GHz local oscillator **506** for generating a 60 GHz carrier signal. The signal generation circuit **504** may also work with other frequencies, such as 70/80 GHz. The 60 GHz signal is output from the local oscillator **506** to a power divider circuit **508** which separates the 60 GHz signal into three separate transmission signals. Each of these separated transmission signals are provided to an IQ mixer **510** that are each connected to one of the layer input connectors **116**. The IQ mixer circuits **510** are connected to an associated additive white gaussian noise circuit **512** for inserting a noise element into the generated transmission signal. The AWG circuit **512** may also generate SuperQAM signals for insertion in to the transmission signals. The IQ mixer **510** generates signals in a manner such as that described in U.S. patent application Ser. No. 14/323,082, filed on Jul. 3, 2014, now U.S. Pat. No. 9,331,875, issued on May 3, 2016, entitled SYSTEM AND METHOD FOR COMMUNICATION USING ORBITAL ANGULAR MOMENTUM WITH MULTIPLE LAYER OVERLAY MODULATION, which is incorporated herein by reference in its entirety.

[0038] Using the transmitter **502** illustrated in FIG. **5**. A multiplexed beam (Hermite Gaussian, Laguerre Gaussian, etc.) can be generated as illustrated in FIG. **6**. As illustrated, the multilayered patch antenna array **102** will generate a multiplexed beam **602** for transmission. In the present example, there is illustrated a multiplex OAM beam that has twists for various order OAM signals in a manner similar to

that disclosed in U.S. patent application Ser. No. 14/323,082. An associated receiver detector would detect the various OAM rings **604** as illustrated each of the rings associated with a separate OAM processed signal.

[0039] When signals are transmitted in free space (vacuum), the signals are transmitted as plane waves. They may be represented as described herein below. Free space comprises a nonconducting medium ($\sigma=0$) and thus $J=\sigma E=0$.

[0040] From experimental results Ampere's law and Faraday's law are represented as:

$$\vec{B}=\mu\vec{H} \quad \nabla xH=\frac{\partial D}{\partial t}+J \quad \text{Ampere's}$$

$$\vec{D}=\in\vec{E}$$

$$\vec{J}=\sigma\vec{E} \quad \nabla xE=\frac{-\partial B}{\partial t} \quad \text{Faraday's}$$

If there is propagation in the z direction and therefore E and H are in the xy plane.

[0041] Without the loss of any generality E may be oriented in the x-direction and H may be oriented in the y-direction thus providing propagation in the z-direction. From Ampere's-Maxwell equation, the following equations are provided:

$$\nabla xH=\frac{\partial D}{\partial t}$$

$$\nabla xH=\begin{vmatrix}\hat{x} & \hat{y} & \hat{z}\\ \frac{\partial}{\partial x} & \frac{\partial}{\partial y} & \frac{\partial}{\partial z}\\ H_x & H_y & H_z\end{vmatrix}$$

$$\left(\frac{\partial Hz}{\partial y}-\frac{\partial Hy}{\partial z}\right)\hat{x}+\left(\frac{\partial Hz}{\partial z}-\frac{\partial Hz}{\partial x}\right)\hat{y}+\left(\frac{\partial Hy}{\partial x}-\frac{\partial Hx}{\partial y}\right)\hat{z}=\frac{\partial}{\partial t}\in E$$

[0042] Next, the vectorial wave equations may be represented as:

$$\nabla xH=\frac{\partial D}{\partial t}+J$$

$$\nabla xH=\in\frac{\partial E}{\partial t}$$

$$\nabla xE=\frac{-\partial B}{\partial t}$$

$$\nabla xE=-\mu\frac{\partial H}{\partial t}$$

$$\nabla xB=0$$

$$\nabla xE=S$$

$$\nabla x\nabla xH=\nabla(\nabla H)-\nabla^2H=-\nabla^2H$$

$$\nabla x\nabla xE=\nabla(\nabla E)-\nabla^2E=-\nabla^2E$$

$$\nabla x(\nabla xH)=\nabla x\left(\in\frac{\partial E}{\partial t}\right)=\in\frac{\partial}{\partial t}(\nabla xE)$$

$$=\in\mu\frac{\partial}{\partial t}\left(\frac{\partial}{\partial t}H\right)$$

-continued

$$\nabla^2H=+\in\mu\frac{\partial^2}{\partial t^2}H$$

$$\nabla^2H-\in\mu\frac{\partial^2}{\partial t^2}H=0$$

$$\nabla x(\nabla xE)=\nabla x\left(-\mu\frac{\partial}{\partial t}H\right)$$

$$=-\mu\frac{\partial}{\partial t}(\nabla xH)$$

$$=-\mu\frac{\partial}{\partial t}\left(\in\frac{\partial E}{\partial t}\right)$$

$$+\nabla^2E=+\mu\in\frac{\partial^2}{\partial t^2}E$$

$$\nabla^2E-\mu\in\frac{\partial^2}{\partial t^1}E=0$$

[0043] Therefore in general:

$$\vec{\nabla}^2\vec{E}+\vec{K}^2\vec{E}=0E(\vec{r},t)$$

$$\vec{E}(r,t)=\vec{E}(\vec{r})e^{-jwt}e^{jkz} \quad \text{Propagating in } z\text{-direction}$$

Therefore:

[0044]

$$\left(\frac{\partial^2}{\partial x^2}+\frac{\partial^2}{\partial y^2}+\frac{\partial^2}{\partial z^2}\right)\vec{E}(\vec{r})e^{-jwt}e^{jkz}+\frac{w^2}{y^2}\vec{E}(\vec{r})e^{-jwt}e^{jkz}=0$$

In free space

$$w=\frac{1}{\sqrt{\mu\in}}=\rightarrow c=\frac{1}{\sqrt{\mu\in o}}$$

$$k^2=\frac{w^2}{c^2}$$

Now:

[0045]

$$\frac{\partial}{\partial z}\vec{E}(\vec{r})e^{jkz}=e^{jkz}\left[\frac{\partial\vec{E}(\vec{r})}{\partial z}+jk\vec{E}(\vec{r})\right]$$

$$\frac{\partial}{\partial z}\vec{E}(\vec{r})e^{jkz}=e^{jkz}\left[\frac{\partial\vec{E}(\vec{r})}{\partial z}+jk\vec{E}(\vec{r})\right]+e^{jkz}\left[\frac{\partial^2\vec{E}(\vec{r})}{\partial z^2}+jk\frac{\partial\vec{E}(\vec{r})}{\partial z}\right]$$

$$=e^{jkz}\left[jk\frac{\partial\vec{E}}{\partial z}-k^2\vec{E}(\vec{r})\right]+e^{jkz}\left[\frac{\partial^2\vec{E}}{\partial z^2}+jk\frac{\partial\vec{E}}{\partial z}\right]$$

Because

[0046]

$$\left|2k\frac{\partial E}{\partial z}\right|\gg\left|\frac{\partial^2E(r)}{\partial z^2}\right|$$

Paraxial assumption

$$\frac{\partial^2 \vec{E}(\vec{r})e^{jkz}}{\partial z^2} = e^{jkz}\left[2jk\frac{\partial^2 \vec{E}(\vec{r})}{\partial z} - k^2\vec{E}(\vec{r})\right]$$

Then:

[0047]

$$\left(\frac{\partial^2}{\partial x^2} + \frac{\partial^2}{\partial y^2} + 2jk\frac{\partial^2}{\partial z}\right)E(x, y, z) = 0$$

Which may be represented in cylindrical coordinates as:

$$\frac{\partial^2}{\partial x^2} + \frac{\partial^2}{\partial y^2} = \frac{1}{q}\frac{\partial}{\partial q}\left(q\frac{\partial}{\partial q}\right) + \frac{1}{q^2}\frac{\partial^2}{\partial \Phi^2}$$

[0048] This provides a paraxial wave equation in cylindrical coordinates:

$$\frac{1}{q}\frac{\partial}{\partial q}\left(q\frac{\partial}{\partial q}\right)E(q, \Phi, z) + \frac{1}{q^2}\frac{\partial^2}{\partial \Phi^2}E(q, \Phi, z) + 2jk\frac{\partial E}{\partial z}(q, \Phi, z) = o$$

$P(z), q(z)$

Then:

[0049]

$$E_0 \sim e^{-j\left[P + \frac{k}{2q}(x^2+y^2)\right]}$$

[0050] In general E_o can rotate on the xy-plane and the wave still propagates in the z-direction.

$$\frac{\partial q}{\partial z} = 1$$

$$\frac{\partial p}{\partial z} = -\frac{j}{q}$$

[0051] q~Curvature of the phase front near the optical axis.

$q_2 = q_1 + z$

where q_2 is the output plane and q_1 is the input plane.∞∞

$$\frac{1}{q} = \frac{1}{R} - j\frac{\lambda}{\pi W^2}$$

where

$$\frac{1}{R}$$

is the curvature of the wavefront intersecting the z-axis.

[0052] Thus for a complete plane wave R=∞, the equation becomes:

$$\frac{1}{q} = \frac{1}{R \to \infty} - j\frac{\lambda}{\pi W^2}$$

$$q_0 = \frac{\pi W^2}{-j\lambda} = \frac{j\pi W_0^2}{\lambda}$$

where W_o is the beam waist.

$$q = q_0 + z = \frac{j\pi W_0^2}{\lambda} + z$$

$$w(z) = w_0\sqrt{1 + \left(\frac{z}{z_r}\right)^2}$$

$$W^2(z) = W_0^2\left[1 + \left(\frac{\lambda z}{\pi W_0^2}\right)^2\right]$$

$$R(z) = z\left[1 + \left(\frac{\pi W_0^2}{\lambda z}\right)^2\right]$$

$$R(z) = z\left[1 + \left(\frac{z_R}{z}\right)^2\right]$$

$$\Phi(z) = \tan^{-1}\left(\frac{z}{z_R}\right)$$

$$\theta = \frac{\lambda}{\pi w_0}$$

$$z = z_R$$

$$w(z) = \sqrt{2}\, w_0$$

[0053] The Rayleigh length is:

$$z_R = \frac{\pi n}{\lambda_0}$$

where n is the index of refraction.

$$w_0^2 = \frac{w^2}{1 + \left(\frac{\pi w^2}{\lambda R}\right)^2}$$

$$z = \frac{R}{1 + \left(\frac{\lambda R}{\pi w^2}\right)^2}$$

[0054] The complex phase shift is represented by:

$$jP(z) = \mathrm{Ln}\left[1 - j\left(\frac{\lambda z}{\pi w_0^2}\right)\right] = \mathrm{Ln}\sqrt{1 + \left(\frac{\lambda z}{\pi w_0^2}\right)^2} - j\tan^{-1}\frac{\lambda z}{\pi w_0^2}$$

[0055] The real part of P(z) represents a phase shift difference between the Gaussian beam and an ideal plane wave. Thus the fundamental mode is provided:

$$E_0(x, y, z) = E_0(r, z)\frac{w_0}{w}e^{-j(jz-\phi)}e^{-r^2\left(\frac{1}{w^2}+\frac{jk}{2R}\right)}$$

where:

$$\phi = \tan^{-1}\frac{\lambda z}{\pi w_0^2}$$

[0056] Higher order modes may also provide other solutions. The solution of rectangular equation:

$$\left(\frac{\partial^2}{\partial x^2}+\frac{\partial^2}{\partial y^2}+2jk\frac{\partial}{\partial z}\right)E(x, y, z) = 0$$

Can be determined in rectangular coordinates to be:

$$E(x, y, z) = \sum_{mn} C_{nm}E_0\frac{w_0}{w(z)}H_m\left[\frac{\sqrt{2}\,x}{w(z)}\right] H_n\left[\frac{\sqrt{2}\,y}{w(z)}\right]e^{\frac{-(x^2+y^2)}{w(t)^2}}e^{-j(m+m+1)\tan^{-1}\frac{z}{z_0}}e^{j\frac{k(x^2+y^2)}{2R(z)}}$$

$$z_0 = \frac{kw_0^2}{2}$$

$$w(z) = w_0\sqrt{1+\frac{z^2}{z_0^2}}$$

$$C_{60} \Rightarrow TEM_{OD}$$

$$R(z) = z+\frac{z_0^2}{z} = \frac{z_0^2}{z}\left(1+\frac{z^2}{z_0^2}\right) = \frac{z_0^2}{zw_0^2}w^2(z) = \frac{kz_0}{2z}w^2(z)$$

[0057] The solution of cylindrical coordinates of equation:

$$\frac{1}{\rho}\frac{\partial}{\partial\rho}\left(\rho\frac{\partial}{\partial\rho}\right)E(\rho, \phi, z)+\frac{1}{\rho^2}\frac{\partial\hat{}\,2E(\rho, \phi, z)}{\delta\phi^2}+2jk\frac{\partial E(\rho, \phi, z)}{\partial z} = 0$$

Can be determined in cylindrical coordinates to be:

$$E(\rho, \phi, z) = \sum_{l\rho} C_{l\rho}E_0\frac{w_0}{w(z)}\left(\frac{\sqrt{2}\,\rho}{w(z)}\right)^l L_l^\rho\left(\frac{\sqrt{2}\,\rho}{w(z)}\right)e^{-\frac{\rho^2}{w^2(t)_e}-j(2\rho+l+1)\tan^{-1}\frac{z}{z_0}}e^{jl\phi}e^{j\frac{k\rho^2}{2R(z)}}$$

The equation

$$L_l^\rho\left(\frac{\sqrt{2\rho}}{w(z)}\right)$$

may also be shown as

$$L_l^\rho\left[\frac{2\rho^2}{w^2(t)}\right].$$

[0058] The lowest mode is the most important mode and in fact this transverse mode is identical for both rectangular and cylindrical coordinates.

$$\varphi(l, P; z) = (2P+l+1)\tan^{-1}\frac{z}{z_0}$$

$$TEM_{00}^{rect} = TEM_{00}^{Cyl}$$

$$C_{00} = 1$$

$$H_0 = 1$$

$$L_0^0 = 1$$

then

$$TEM_{00} \Rightarrow E(\rho, z) \sim E_0\frac{w_0}{w(z)}e^{-\frac{\rho^2}{w^2(t)}}e^{-j\tan^{-1}\frac{z}{z_0}}e^{jk\frac{\rho^2}{2R(z)}}$$

[0059] Referring now to FIG. **7**, there is illustrated a receiver **702** for demultiplexing signals received from a multiplexed signal generated using the transmitter **502** of FIG. **5**. The receiver **702** includes a multilayer patch antenna array **102** such as that described herein above. The multilayer patch antenna array **102** receives the incoming multiplexed signal **704** and each layer **104**, **106**, **108** of the antenna array **102** will extract a particular order of the received multiplexed signal from each of the connector outputs **116** of a particular layer. The signals from each of the connectors **116** are applied to a mixer circuit **706** that demultiplexes the received signal in a manner similar to that discussed with respect to U.S. patent application Ser. No. 14/323,082 using a 60 GHz local oscillator signal from oscillator **708**. The demultiplexed signal may then be read using, for example, a real-time oscilloscope **710** or other signal reading device. Each of the three transmitted signals is thus decoded at the receiver **702** that were transmitted in each of the ordered OAM signals received from the transmitters **602**. In a further embodiment, a demultiplexing approach using SPP (spiral phase plate) may also be applied to detect OAM channels.

[0060] The signals transmitted by the transmitter **502** or the receiver **702** may be used for the transmission of information between two locations in a variety of matters. These include there use in both front haul communications and back haul communications within a telecommunications or data network.

[0061] Referring now more particularly to FIG. **8**, there is illustrated a patch antenna element **110**. Multiple ones of these patch antenna elements **110** are located upon the multilayer patch antenna array **102** as discussed hereinabove. The antenna element **110** includes a patch **802** having a length L and a width W. The patch **802** is fed from an input transmission line **804** that is connected with the feed network **104** (FIG. **1**) and is resting upon a substrate **806** having a height h. The microstrip patch antenna includes a first radiating slot **808** along a first edge of the patch **802** and a second radiating slot **810** along a second edge of the patch

802. The electronic field at the aperture of each slot can be decomposed into X and Y components as illustrated in FIG. **9**. The Y components are out of phase and cancel out because of the half wavelength transmission line **804**. The radiating fields can be determined by treating the antenna as an aperture **900** as shown in FIG. **9** having a width W **902** and a height h **904**.

[0062] The transmission line model can be further analyzed in the following manner. G_r is the slot conductance and B_r is the slot susceptance. They may be determined according to the equations:

$$G_r = \begin{cases} \frac{W^2}{90\lambda_0^2} & \text{for } W < \lambda_0 \\ \frac{W}{120\lambda_0} & \text{for } W > \lambda_0 \end{cases}$$

$$B_r = \frac{2\pi\Delta l\sqrt{\varepsilon_{eff}}}{\lambda_0 Z_0}$$

[0063] The input admittance of the patch antenna **110** can be approximated as:

$$Y_{in} = Y_{slot} + Y_0\frac{Y_{slot} + jY_0\tan(\beta(L+2\Delta l))}{Y_0 + jY_{slot}\tan(\beta(L+2\Delta l))}$$

where Δl is the end effect of the microstrip.

The rectangular patch antenna **110** will resonate when the imaginary part of the input admittance goes to zero.

[0064] The end effect may be calculated according to the equation:

$$\Delta l = 0.412h\left(\frac{\varepsilon_{eff}+0.3}{\varepsilon_{eff}-0.258}\right)\frac{(W/h)+0.264}{(W/h)+0.8}$$

$$L + 2\Delta l = \frac{\lambda_g}{2} = \frac{\lambda_0}{2\sqrt{\varepsilon_{eff}}}$$

$$\varepsilon_{eff} = \frac{\varepsilon_r+1}{2} + \frac{\varepsilon_r-1}{2}\left(1+\frac{10h}{W}\right)^{-0.5}$$

[0065] The resonant frequency of the patch antenna **110** is given by:

$$f_r = \frac{C}{2\sqrt{\varepsilon_{eff}}\,(L+2\Delta l)}$$

Typically the width W of the aperture is given by:

$$W = \frac{c}{2f_r}\left(\frac{\varepsilon_r+1}{2}\right)^{-1/2}$$

[0066] The multilayered patch antenna array **102** may transmit both Hermite Gaussian beams using the processing discussed with respect to U.S. patent application Ser. No. 14/323,082 or Laguerre Gaussian beams. When transmitting Laguerre Gaussian beams information may be transmitted in a number of fashions. A spiral phase plate and beam splitter approach may be used, a dual OAM mode antenna approach may be used or the patched antenna described herein may be utilized. These implementations would be beneficial in both fronthaul and backhaul applications.

[0067] In order to transmit several OAM modes of order l and amplitude a_l^{OAM}, the antenna elements must be fed by an input signal according to the equation:

$$a_n^{feed}\frac{1}{\sqrt{N}}\sum_{l=0}^{N-1} a_l^{OAM} e^{-j2\pi\frac{ln}{N}},\ n\in\{0,\ldots,N-1\},$$

[0068] Note that the number of elements in the multilayer patch antenna array **102** limits the number of possible OAM modes due to sampling. Due to aliasing, modes of order greater than N/2 are actually modes of negative orders.

$$b_{l'}^{OAM} = \frac{1}{\sqrt{N}}\sum_{p=0}^{N-1} b_p^{feed} e^{j2\pi\frac{pl'}{N}},\ p\in\{0,\ldots,N-1\},$$

$$h_{pn} = \beta e^{-jkr_{np}}\frac{\lambda}{4\pi r_{np}},$$

$$r_{pn} = \sqrt{D^2 + R_t^2 + R_r^2 - 2R_tR_r\cos(\theta_{np})},$$

$$\theta_{pn} = 2\pi\left(\frac{n-P}{N}\right),$$

$$\beta = \sqrt{g_t g_r}$$

Single Mode Link Budget

[0069]

$$H_{tot} = U^H H U$$

$$b^{OAM} = H_{tot}a^{OAM}$$

$$\frac{P_r}{P_t}(l) = \left|\frac{b_l^{OAM}}{a_l^{OAM}}\right|^2 = \left|\sum_{p=0}^{N-1}\sum_{n=0}^{N-1}\frac{\beta}{N}e^{-jl\theta_{np}}e^{-jkr_{np}}\frac{\lambda}{4\pi r_{np}}\right|^2$$

Asymptotic Formulation

[0070] The object is to determine an asymptotic formulation of the Link budget at large distances, i.e. when D→+(∞), we seek the leading term for each value of 1 Link budget−1 are the same.

[0071] The link budget is asymptotically given by:

$$\frac{P_r}{P_t}(|l|) = \left|\frac{\lambda\beta}{4\pi|l|!}\left(\frac{kR_tR_r}{2}\right)^{|l|}\frac{1}{D^{|l|+1}}\right|^2$$

[0072] From the Fraunhofer distance $2(2\max(R_t,R_r))^2/\lambda=200\lambda$, the link budget asymptotically tends to straight lines of slope −20 (|l|+1) dB per decade, which is consistent with an attenuation in $1/D^{2|l|+2}$.

Asymptotic Expressions with Gains and Free Space Losses

[0073] Gains and free space losses may be determined by:

$$\frac{P_r}{P_t}(|l|) = \frac{Ng_t}{|l|!}\left(\frac{4\pi(\pi R_t^2)}{\lambda^2}\right)^{|l|}\frac{Ng_r}{|l|!}\left(\frac{4\pi(\pi R_t^2)}{\lambda^2}\right)^{|l|}\left(\frac{\lambda}{4\pi D}\right)^{2|l|+2}$$

$$L_{FS_{eq}}(l) = \left(\frac{4\pi D}{\lambda}\right)^{2|l|+2}$$

$$G_{eq}(l) = \frac{Ng}{|l|!}\left(\frac{4\pi(\pi R^2)}{\lambda^2}\right)^{|l|}$$

[0074] For a fixed value of |l|, each equivalent gain increases $R^{2|l|}$ So that the link budget improves by a factor of $R^{4|l|}$. On the contrary, for a fixed value of R, when |l| increases, the link budget decreases since asymptotically the effect of D is greater than those of R_t and R_r.

[0075] Referring now to FIG. **10**, there is illustrated a 3-D model of a single rectangular patch antenna designed for 2.42 GHz and only one linear polarization. The radiation pattern for this antenna is illustrated in FIG. **11**.

[0076] FIG. **12***a* illustrates the radiation patterns of the circular array for an OAM mode order l=0 due to the higher grating lobes. FIGS. **12***b*, **12***c* and **12***d* illustrate the radiation patterns for the OAM mode orders in l=0 (FIG. **12***b*), l=1 (FIG. **12***c*), and l=2 (FIG. **12***d*) in the vicinity of the array axis.

[0077] Asymptotic OAM path loss is illustrated by:

$$\frac{P_r}{P_t}(|l|) = \frac{Ng_t}{|l|!}\left(\frac{4\pi(\pi R_t^2)}{\lambda^2}\right)^{|l|}\frac{Ng_r}{|l|!}\left(\frac{4\pi(\pi R_t^2)}{\lambda^2}\right)^{|l|}\left(\frac{\lambda}{4\pi D}\right)^{2|l|+2}$$

When assuming e-band frequencies, a distance of 1000 m and a reasonable patch antenna element gains, other parameters may be calculated including the diameter for the transmitter and receiver array rings, number of antennas, etc.

[0078] FIG. **13** illustrates the use of a multilevel patch antenna array in a parabolic antenna **1302**. The multilevel patch antenna array **102** is positioned at the focus point of a parabolic reflector **1306** to radiate its output signal **1304** to reflect off of the parabolic reflector **1306**. The patch antenna array **102** is mounted to the parabolic reflector **1302** via structural support members **1308**. The parabolic reflector **1306** reflects the multiplexed beam that may then be detected at some type of receiving antenna. The approach has been shown to provide a higher gain output for the antenna over one only including a multilevel patch antenna array **102** without a parabolic reflector **1306**.

[0079] Referring now to FIG. **14**, there are illustrated a number of implementations using the multilevel patch antenna array **102** and parabolic reflector **1306**. In the axial or FriendFeed implementation **1402**, the patch antenna array **102** is positioned at the focal point of the parabolic reflector **1306** by the supports **1308** to radiate signals directly into the parabolic reflector **1306** along a central axis **1404**. The reflected beam will then come straight off of the parabolic reflector **1306** and parallel to each other. If the patch antenna array is moved by an offset O form the focal point away from the parabolic reflector **1306**, the reflected beam from the parabolic reflector will focus at a particular point. In this manner by moving the array along the axis of the focus point the reflected beam can be focused at desired points along the axis. The off axis or offset feed approach **1406** positions the patch antenna array **102** off of the central axis **1404** to radiate the beam at an angle to the central axis **1404** to reflect off of the parabolic reflector **1306**. The patch antenna array **102** is held in its off axis position by support member **1308**.

[0080] In the Cassegrain configuration **1408**, the multilevel patch antenna array **102** is positioned on the primary parabolic reflector **1306** and reflects outward toward a convex secondary reflector **1410** held in place by secondary reflector support members **1412**. The radiated signal reflects off of the convex reflector **1410** at an angle similar to the off axis reflection of implementation **1406** and reflects a second time off the surface of the parabolic reflector **1306**.

[0081] Finally, the Gregorian implementation **1414** mounts the multilevel patch antenna array **102** on the surface of the parabolic reflector **1306** to project outward toward a concave secondary reflector **1416**. The secondary reflector **1416** is supported by secondary reflector supports **1418**. The signal radiated by the multilevel patch antenna array **102** reflects off of the secondary reflector **1416**, and a second time off of the primary parabolic reflector **1306**. Each of these cases direct the Hermite Gaussian, Laguerre Gaussian, orthogonal function multiplexed beam outward toward a receiver.

[0082] The asymptotic OAM path loss using a parabolic antenna revises the previous loss equations in the following manner:

$$\frac{P_r}{P_t}(|l|) = \frac{Ng_t}{|l|!}\left(\frac{4\pi(\pi R_t^2)}{\lambda^2}\right)^{|l|}\frac{Ng_r}{|l|!}\left(\frac{4\pi(\pi R_t^2)}{\lambda^2}\right)^{|l|}\left(\frac{\lambda}{4\pi D}\right)^{2|l|+2}G_{New}$$

The term G_{New} comprises the new variable arising due to the parabolic antenna. As previously discussed, assuming e-band frequencies, a distance of 1000 m and a reasonable patch antenna element gains, other parameters may be calculated including the diameter for the transmitter and receiver array rings, number of antennas, etc.

[0083] The new loss equation may be further solved in the following manner:

$$\frac{P_r}{P_t}(|l|) = \frac{Ng_t}{|l|!}\left(\frac{4\pi(\pi R_t^2)}{\lambda^2}\right)^{|l|}\frac{Ng_r}{|l|!}\left(\frac{4\pi(\pi R_t^2)}{\lambda^2}\right)^{|l|}\left(\frac{\lambda}{4\pi D}\right)^{2|l|+2}G_{New}$$

$$G_{New} = \frac{4\pi(\pi R_A^2)}{\lambda^2}e_A$$

$$\frac{P_r}{P_t}(|l|) = \frac{Ng_t}{|l|!}\left(\frac{4\pi(\pi R_t^2)}{\lambda^2}\right)^{|l|}\frac{Ng_r}{|l|!}\left(\frac{4\pi(\pi R_t^2)}{\lambda^2}\right)^{|l|}\left(\frac{\lambda}{4\pi D}\right)^{2|l|+2}\frac{4\pi(\pi R_A^2)}{\lambda^2}e_A$$

Where R equals the radius of the parabolic antenna and e_A is the aperture efficiency of the parabolic antenna 0.55 to 0.70.

[0084] Referring now to FIG. **15**, a hybrid patch antenna **1502** and parabolic reflector **1504** uses a single reflection to generate an OAM beam. The patch antenna **1502** is placed at the focal point of the parabolic reflector **1504**. As discussed previously, the case of double reflection wherein the patch antenna **1502** is placed at the feed of a Cassegrain antenna (see FIG. **14** reference number **1408** and **1414**) and the generated OAM beams are reflected twice by a sub reflector and by the parabolic reflector. FIG. **16** illustrates simulated power as a function of a transmission distance

considering both the OAM beam divergence as well as the blocking affect of a patch antenna. All the power in the example illustrated in FIG. **16** is normalized to the total power covered by the parabolic reflector. In the example illustrated in FIG. **16**, the parabolic reflector is 4 feet in diameter.

[0085] The receiver sensitivities of commercially available millimeterwave communications systems have been reviewed as listed below in Table A. The potential transmission distance of using a hybrid patch antenna and parabolic dish as the transmitter taking into consideration the commercially available receiver sensitivities is illustrated.

					Estimated distance of our approach in this commercial system (transmitter power, parabolic dish diameter)			
Company	Model	Frequency	Highest data rate	Receiver sensitivity	10 dBm, 4 feet	30 dBm, 4 feet	10 dBm, 8 feet	30 dBm, 8 feet
Fujitsu	GX4000	70/80 GHz	3 Gbps	−54 dBm	1 km for OAM 1, 400 m for OAM 2	1.8 km for OAM 1, 700 m for OAM 2	1.8 km for OAM 1, 1.2 km for OAM 2	>3 km for OAM 1, 2 km for OAM 2
E-band communications	E-Link 1000Q	70/80 GHz	1.25 Gbps	−66 dBm	1.4 km for OAM 1, 500 m for OAM 2	2.5 km for OAM 1, 800 m for OAM 2	2.5 km for OAM 1, 1.6 km for OAM 2	>3 km for OAM 1, 2.5 km for OAM 2
	E-Link Eagle	70/80 GHz	3 Gbps	−48 dBm (estimated)	800 m for OAM1, 350 m for OAM2	1.5 km for OAM 1, 500 m for OAM 2	1.5 km for OAM 1, 1 km for OAM 2	3 km for OAM 1, 1.7 km for OAM 2
Bridge Wave	GE60	60 GHz	1 Gbps	−60 dBm (estimated)	1.2 km for OAM 1, 400 m for OAM 2	2.2 km for OAM 1, 700 m for OAM 2	2.2 km for OAM 1, 1.5 km for OAM 2	>3 km for OAM 1, 2.2 km for OAM 2
	AR60	60 GHz	1 Gbps	−60 dBm (estimated)	1.2 km for OAM 1, 400 m for OAM 2	2.2 km for OAM 1, 700 m for OAM 2	2.2 km for OAM 1, 1.5 km for OAM 2	>3 km for OAM 1, 2.2 km for OAM 2
	AR60X	60 GHz	1 Gbps	−70 dBm (estimated)	1.6 km for OAM 1, 600 m for OAM 2	3 km for OAM1, 900 m for OAM 2	>3 km for OAM 1, 1.8 km for OAM 2	>3 km for OAM 1, 3 km for OAM 2

[0086] FIG. **17** illustrates a configuration for an OAM multiplexed 60 GHz link using a hybrid patch and parabolic antenna **1702**. The receivers **1704** are configured with spiral phase plates **1706** and focusing lens **1708**. The spiral phase plate **1706** demultiplexes the received OAM signals. FIG. **18** illustrates another hybrid patch parabolic antenna configuration that includes a hybrid patch and parabolic antenna for both the transmitter **1802** and receiver **1804** with no beam splitters. The configurations of FIGS. **17** and **18** will use 60 GHz millimeter wave data links to multiplex OAM+1 and OAM−2 using the hybrid patch and parabolic antennas. The system using the hybrid patch and parabolic antennas will provide kilometer transmission distances.

[0087] The production of the patch antennas **110** are carried out through a design and layout process as generally illustrated in FIG. **19**, a clean room procedure for production of the antenna as generally illustrated in FIG. **20** and a final testing process as illustrated in FIG. **21**. Referring now to FIG. **19**, the design and layout process is more particularly described. Initially, the patch antenna is designed and simulated at step **1902** using ANSYS HFSS with a microstrip feed structure. ANSYS HFSS comprises a high-frequency structural simulator. The software within the device stimulates 3-D full wave electromagnetic field. The ANSYS HFSS creates a GDSII file (graphic database system file used to control integrated circuit photomask plotting) from the HFSS simulation and exports the GDSII file to an AWR (Applied Wave Research Corporation) Microwave Office (MWO) layout at step **1904**. In order to measure the antenna with ground signal ground probe feeding, a previously design conductor backed coplanar waveguide to microstrip transition design that has been fabricated using Agilent Momentum is also imported at step **1906** as a GDSII Agilent Momentum file into the AWR MWO Layout. The two designs are brought together at step **1908** and a weight and etch compensation of 12 μm is added to the lateral dimensions to account for isotropic wet etch used in the fabrication process. The final GDSII file for the layout is exported at step **1910** and provided to a clean room for fabrication at step **1912**.

[0088] Referring now to FIG. **20**, there is illustrated the clean room process for patterning a copper layer on the FR408 laminate. Initially, the double-sided Cu FR408 laminate is cut using scissors at step **2002** to an appropriate size (typically 1.5"×1.5"). The FR408 laminate is cleaned by rinsing the laminate at step **2004** with acetone, isopropanol (IPA) and nitrogen (N_2) and dried in a solvent hood or using program 2 of a CPK Solvent Spinner with the appropriate chuck. The laminate is dehydrate baked at 130° C. for two minutes on a hot plate (for example, a Cole Parmer digital hotplate) at step **2006**. Next, at step **2008**, hexamethyldisilizane (HMDS) is deposited on the laminate by a rain method using a Yield Engineering YES—**310** vacuum hood oven. The laminate samples are placed in the HMDS oven for 20 minutes to improve resist adhesion. Next, at step **2010**, the mask is cleaned using program 2 of a CPK Solvent Spinner with the appropriate chuck. The mask is further cleaned using an automated mask cleaner (Ultratech Mask Cleaner) using program 0 DIW only at step **2012**.

[0089] The lithography process is performed at steps **2014-2034**. First, Shipley S1813 photoresist is spun on to the backside of the laminate at step **2014** to protect the ground layer using for example a Brewer Science Cee Spin Coater System. In one embodiment, the spin coater system will operate at 3000 rpm with 3000 rpm/s for 60 seconds. The sample is soft baked at step **2016** at 115° C. for 90 seconds on a hot plate and hard baked at step **2018** at 130° C. for 60 seconds on the hotplate. S1813 resist is spun onto the top side pattern copper layer at step **2022**. In one embodiment, this is carried out at 3000 rpm with 3000 rpm/s for 60 seconds. The sample is soft baked at 115° C. for 90 seconds on a hot plate at step **2022**. The top side of the sample is exposed at step **2024** with 110 mJ/cm2 using Karl Suss MA6 BA6 Contact Aligner/Printer. Next, the circuit is developed at step **2026** with Microposit MF-319 for 60 seconds in a beaker. The sample is rinsed with deionized water (DIW) and N_2 in a base hood. A reactive ion etching process is performed at step **2032** to remove excess photoresist using Techniques Series 85 RIE. This is achieved by applying O_2 only at 180 mTorr with 50 W for 15 seconds. The sample is hard baked at step **2034** at 130° C. for 60 seconds on a hot plate. The lithography is checked at step **2036** under a Leica Inm Optical microscope to make sure the lithography is correct and that the gaps are defined and not overdeveloped.

[0090] The 12 μm copper layer is etched at steps **2038-2046**. The copper is etched in one minute intervals at step **2038** by agitating the sample in a Cu etchant. Inquiry step **2040** determines if the Cu etching process is complete, and if not, the sample is rotated at step **2042** by 90° and returns to agitate the sample within the Cu etchant at step **2038**. When inquiry step **2040** determines that the Cu etching process is completed control passes to step **2044** wherein the sample is rinsed with DIW and N_2 and dried within a base hood. The sample is checked at inquiry step **2046** using a microscope to determine if the Cu has been completely removed. If not, control passes back to step **2038** for further agitation within the Cu etchant. If all of the Cu has been removed control passes to the stripping of the photoresist process.

[0091] The stripping of the photoresist occurs by first rinsing the sample with acetone, IPA, DIW and N_2 and drying within a solvent hood or using program 2 in CPK Solvent Spinner with the appropriate chuck. The sample is dehydrate baked at step **2050** at 130° C. for five minutes on a hot plate. The etched laminate samples are examined at step **2052** under a microscope to make sure that gaps are etched with no over etching of areas within the sample.

[0092] The created patch antenna may be tested as illustrated in FIG. **21** to confirm operation of the antenna. Initially, at step **2102**, a DC test is performed upon the antenna to make sure that the G-S-G feed is not shorted. An RF test is performed at step **2104** to measure the S_{11}-Return Loss across the frequency bands using Agilent VNA on Cascade M150 probe station. The radiation pattern of the antenna may then be measured at step **2106** at the appropriate frequencies using a NSI spherical near field scanner.

[0093] It will be appreciated by those skilled in the art having the benefit of this disclosure that this patch antenna array for transmission of Hermite-Gaussian and Laguerre-Gaussian beams provides for the transmission of multiplexed Hermite Gaussian and Laguerre Gaussian modes in a single transmission beam. It should be understood that the drawings and detailed description herein are to be regarded in an illustrative rather than a restrictive manner, and are not intended to be limiting to the particular forms and examples disclosed. On the contrary, included are any further modifications, changes, rearrangements, substitutions, alternatives, design choices, and embodiments apparent to those of ordinary skill in the art, without departing from the spirit and scope hereof, as defined by the following claims. Thus, it is intended that the following claims be interpreted to embrace all such further modifications, changes, rearrangements, substitutions, alternatives, design choices, and embodiments.

What is claimed is:

1. A multi-level antenna array, comprising:

a plurality of patch antennas;

a plurality of layers, each of the plurality of layers separated from each other by a distance, each of the plurality of layers further supporting a portion of the plurality of patch antennas;

a plurality of connectors, each of the plurality of connectors associated with one of the plurality of layers, for supplying a signal for transmission by the associated layer;

a feed network on each of the plurality of layers for providing a connection between a connector of the plurality of connectors associated with the layer and the portion of the plurality of patch antennas located on the layer;

wherein each layer of the plurality of layers transmits the signal having a different orthogonal function applied thereto that multiplexes each of the signals having a different orthogonal function applied thereto onto a single transmission beam; and

a parabolic reflector for reflecting the single transmission beam from the plurality of layers of the multi-level antenna array.

2. The multi-level antenna array of claim **1** further including a secondary reflector for receiving the single transmission beam from the plurality of layers of the multi-level antenna array and directing the single transmission beam toward the parabolic reflector.

3. The multi-level antenna array of claim **1**, wherein the plurality of layers of the multi-level antenna array are placed at a focal point of the parabolic reflector.

4. The multi-level antenna array of claim **1**, wherein the different orthogonal function comprises one of a Hermite-Gaussian function, a Laguerre-Gaussian function or an Ince-Gaussian function.

5. The multi-level antenna array of claim **1**, wherein the plurality of patch antennas in each of the plurality of layers are configured in at least one of a rectangular, circular or elliptical configuration.

6. The multi-level antenna array of claim **1**, wherein each of the plurality of a patch antennas on a layer of the plurality of layers have a different phase applied thereto.

7. The multi-level antenna array of claim **1**, wherein the single transmission beam is transmitted on a single frequency.

8. The multi-level antenna array of claim **1**, wherein the different orthogonal function comprises one of a Jacobi polynomial function, Gegenbauer polynomial function, Legendre polynomial function, Chebyshev polynomial function, Legendre function, Bessel function or prolate spheroidal function.

9. A system for transmitting a transmission beam comprising:

a transmitter including a first multi-level patch antenna array for modulating and transmitting the transmission beam, the first multi-level patch antenna array further comprising:

a first plurality of patch antennas;

a first plurality of layers, each of the first plurality of layers separated from each other by a distance, each of the first plurality of layers further supporting a portion of the first plurality of patch antennas;

a first plurality of connectors, each of the first plurality of connectors associated with one of the first plurality of layers, for supplying a signal for transmission by the associated layer;

a first feed network on each of the first plurality of layers for providing a connection between a first connector of the first plurality of connectors associated with the layer and the portion of the first plurality of patch antennas located on the layer;

wherein each layer of the first plurality of layers transmits the signal having a different orthogonal function applied thereto that multiplexes each of the signals having a different orthogonal function applied thereto onto a single transmission beam; and

a first parabolic reflector for reflecting the single transmission beam from the first plurality of layers of the multi-level antenna array;

a receiver including a second multi-level patch antenna array for receiving and demodulating the transmission beam, the second multi-level patch antenna array further comprising:

a second plurality of patch antennas;

a second plurality of layers, each of the second plurality of layers separated from each other by a distance, each of the second plurality of layers further supporting a portion of the second plurality of patch antennas;

a second plurality of connectors, each of the second plurality of connectors associated with one of the second plurality of layers, for supplying a signal for transmission by the associated layer;

a second feed network on each of the second plurality of layers for providing a connection between a connector of the second plurality of connectors associated with the layer and the portion of the second plurality of patch antennas located on the layer;

wherein each layer of the second plurality of layers receives the signal having a different orthogonal function applied thereto that demultiplexes each of the signals having the different orthogonal function applied from the single transmission beam; and

a parabolic reflector for reflecting the single transmission beam to the plurality of layers of the multi-level antenna array.

10. The system of claim 9 further including a secondary reflector for receiving the single transmission beam from the first plurality of layers of the multi-level antenna array and directing the single transmission beam toward the first parabolic reflector.

11. The system of claim 9, wherein the first plurality of layers of the multi-level antenna array are placed at a focal point of the first parabolic reflector.

12. The system of claim 9, wherein the different orthogonal function comprises one of a Hermite-Gaussian function, a Laguerre-Gaussian function or an Ince-Gaussian function.

13. The system of claim 9, wherein the first plurality of patch antennas in each of the first plurality of layers are configured in at least one of a rectangular, circular or elliptical configuration.

14. The system of claim 9, wherein each of the first plurality of a patch antennas on a layer of the first plurality of layers have a different phase applied thereto.

15. The system of claim 9, wherein the single transmission beam is transmitted on a single frequency.

16. The system of claim 9, wherein the different orthogonal function comprises one of a Jacobi polynomial function, Gegenbauer polynomial function, Legendre polynomial function, Chebyshev polynomial function, Legendre function, Bessel function or prolate spheroidal functions.

17. A multi-level antenna array, comprising:

a plurality of patch antennas;

a plurality of layers, each of the plurality of layers separated from each other by a distance, each of the plurality of layers further supporting a portion of the plurality of patch antennas;

a plurality of connectors, each of the plurality of connectors associated with one of the plurality of layers, for supplying a signal for transmission by the associated layer;

a feed network on each of the plurality of layers for providing a connection between a connector of the plurality of connectors associated with the layer and the portion of the plurality of patch antennas located on the layer;

wherein each layer of the plurality of layers transmits the signal having a different orthogonal function applied thereto that multiplexes each of the signals having a different orthogonal function applied thereto onto a single transmission beam.

18. The multi-level antenna array of claim 17, wherein the different orthogonal function comprises one of a Hermite-Gaussian function, a Laguerre-Gaussian function or an Ince-Gaussian function.

19. The multi-level antenna array of claim 17, wherein the plurality of patch antennas in each of the plurality of layers are configured in at least one of a rectangular, circular or elliptical configuration.

20. The multi-level antenna array of claim 17, wherein each of the plurality of a patch antennas on a layer of the plurality of layers have a different phase applied thereto.

21. The multi-level antenna array of claim 17, wherein the single transmission beam is transmitted on a single frequency.

22. The multi-level antenna array of claim 17, wherein the different orthogonal function comprises one of a Jacobi polynomial function, Gegenbauer polynomial function, Legendre polynomial function, Chebyshev polynomial function, Legendre function, Bessel function or prolate spheroidal functions.

* * * * *